Shelf-basin exchange times of Arctic surface waters estimated from $^{228}Th/^{228}Ra$ disequilibrium

M. Rutgers van der Loeff[1], P. Cai[1,2], I. Stimac[1], D. Bauch[3], C. Hanfland[1], T. Roeske[1] and S.B. Moran[4]

[1]Alfred-Wegener Institute for Polar and Marine Research, D27570 Bremerhaven, Germany

[2]State Key Laboratory of Marine Environmental Science, Xiamen University, Xiamen 361005, China

[3]Leibniz Institute of Marine Sciences at University Kiel (IFM-GEOMAR), D24148 Kiel, Germany

[4]Gradulate School of Oceanography, University of Rhode Island, Narragansett, Rhode Island, USA

Keywords: Radium isotopes, Arctic Ocean, GEOTRACES, natural radionuclides

*Corresponding author:

Michiel Rutgers van der Loeff

Alfred Wegener Institute for Polar and Marine Research

PO Box 120161, D 27515 Bremerhaven, Germany

E-mail: mloeff@awi.de

Phone: +49 471 4831 1259

Fax: +49 471 4831 1425

Abstract

The Trans Polar Drift is strongly enriched in ^{228}Ra accumulated on the wide Arctic shelves with subsequent rapid off-shore transport. We present new data of Polarstern expeditions to the central Arctic and to the Kara and Laptev Seas. Because ^{226}Ra activities in Pacific waters are 30% higher than in Atlantic waters, we correct ^{226}Ra for the Pacific admixture when normalizing ^{228}Ra with ^{226}Ra. The use of ^{228}Ra decay as age marker critically depends on the constancy in space and time of the source activity, a condition that has not yet adequately been tested. While ^{228}Ra decays during transit over the central Basin, ingrowth of ^{228}Th could provide an alternative age marker. The high ^{228}Th/^{228}Ra activity ratio (AR=0.8 – 1.0) in the central basins is incompatible with a mixing model based on horizontal eddy diffusion. An advective model predicts that ^{228}Th grows to an equilibrium AR, the value of which depends on the scavenging regime. The low AR over the Lomonosov Ridge (AR=0.5) can be due to either rapid transport (minimum age without scavenging 1.1 year) or enhanced scavenging. Suspended particulate matter (SPM) load (derived from beam transmission and particulate ^{234}Th) and total ^{234}Th depletion data show that scavenging, although extremely low in the central Arctic, is enhanced over the Lomonosov Ridge, making an age of 3 yr more likely. The combined data of ^{228}Ra decay and ^{228}Th ingrowth confirm the existence of a recirculating gyre in the surface water of the eastern Eurasian Basin with a river water residence time of at least 3 years.

1. INTRODUCTION

The Arctic Ocean comprises just 1% of World Ocean volume but receives 10% of World river discharge. Surface water with a large river water component and imprints from the wide shelf areas are carried across the central Arctic in the Trans Polar Drift (TPD). With the rapid reduction of summer ice cover in the deep central Arctic major changes can be expected in primary production and biogeochemical cycles. How the central Arctic ecosystem will develop will strongly depend on the composition and circulation of the surface water. It is therefore important to quantify the rate and mode of surface water exchange between shelves and central basins. The circulation of surface waters in the central Arctic is not known as accurately as we know the ice drift. It took the ice 2.9 y to carry Nansen's *Fram* from the Laptev Sea before leaving the Arctic at 80°N, but with 1979-2006 climatology this drift would on average have taken 3.7y (PFIRMAN et al., 2009). The rapid drift of *Tara* in the years 2006-2008 (ca 1.5 years, DAMOCLES Project) shows that the ice drift has lately accelerated, as is also documented by numerous buoys deployed in the ice and tracked by satellite (International Arctic Buoy Programme). The surface water residence time, which needs not be the same as that of the ice, was estimated by Schlosser et al. (1999) to be 2-5 yr, but these authors mention that their method (tritium/^{3}He ages) gives a minimum estimate because of possible losses of ^{3}He to the atmosphere through leads in the ice. The residence time of freshwater in the Arctic is approximately 10 years (SERREZE et al., 2006).

The natural radionuclide ^{228}Ra is a powerful tracer for shelf inputs to the open ocean (MOORE et al., 1986) and is particularly well suited for such studies in the Arctic Ocean, which comprises 25% of the World shelf areas. Earlier ^{228}Ra measurements from 1991 (RUTGERS

69 VAN DER LOEFF et al., 1995) and 1994 (SMITH et al., 2003) showed high surface water ^{228}Ra
70 activities in the TPD. Kadko and Muench (2005) confirmed low ^{228}Ra/^{226}Ra in the Beaufort
71 Gyre due to decay during the long residence time in this basin. Hansell et al. (2004) and
72 Letscher et al. (2011) used this decay to derive decomposition rates of dissolved organic
73 carbon. Kadko and Aagaard (2009) derived water mass ages of halocline waters using
74 submarine-collected samples. This use of the decay of ^{228}Ra to derive the time since a water
75 parcel left the shelf is critically dependent on the assumption that the ^{228}Ra activity of waters,
76 when they leave contact with the shelf, is known and constant over time and space. This has
77 not been tested yet. In fact, there are indications that there are differences between individual
78 shelf areas (RUTGERS VAN DER LOEFF et al., 2003). Indications of a systematic difference
79 between Eurasian and American shelf concentrations (SMITH et al., 2003) were not supported
80 by Kadko and Muench (2005) who argue that their data from the Chukchi are in accord with
81 published distributions in the Eurasian Arctic.
82
83 The general circulation of surface waters in the Arctic Ocean is characterized by an
84 anticyclonic (clockwise) circulation in the Beaufort Gyre and a cyclonic circulation in the
85 Eurasian Basin. The two systems meet in the TPD (PFIRMAN et al., 1997; RUDELS, 2009)
86 which forms the transition between waters of Pacific and Atlantic origin. Depending on the
87 Arctic Oscillation the general circulation changes between periods with stronger cyclonic or
88 anticyclonic character (PROSHUTINSKY and JOHNSON, 1997). In the 1990s, a strong change
89 towards cyclonic circulation weakened the Beaufort Gyre and the Atlantic/Pacific front
90 shifted from approximately the Lomonosov to the Alpha/Mendeleev Ridges (MCLAUGHLIN
91 et al., 1996; EKWURZEL et al., 2001), which resulted in a shift in the geographic positions of

maximum ^{228}Ra concentrations (SMITH et al., 2003). Such changes in surface circulation likely change the residence time of water over the shelves and may therefore also have changed the accumulated ^{228}Ra activities. While ^{228}Ra may thus be a useful tracer for the variability in the outflow of shelf water from the Laptev Sea (SMITH et al., 2003), the calculation of surface water age from ^{228}Ra activities becomes questionable. It is therefore desirable to have additional tracers of the transit time of water in the TPD.

The ingrowth of ^{228}Th into its parent ^{228}Ra could serve that purpose. We know from studies of ^{234}Th that thorium is effectively removed on the shelves (Barents Sea: (COPPOLA et al., 2002; RUTGERS VAN DER LOEFF et al., 2002); Chukchi Sea: (MORAN et al., 1997; MORAN et al., 2005; LALANDE et al., 2007; LEPORE et al., 2007); Beaufort Sea (MORAN and SMITH, 2000), Laptev Sea (CAI et al., 2010)). These high thorium scavenging rates also cause ^{228}Th to be depleted with respect to ^{228}Ra (TRIMBLE et al., 2004; LEPORE and MORAN, 2007). In the Canada Basin thorium scavenging rates decrease northward (MORAN et al., 1997; TRIMBLE et al., 2004; TRIMBLE and BASKARAN, 2005) and reach very low values on the Alpha Ridge in the central Arctic (BACON et al., 1989). Indeed, in large areas of the central Arctic, scavenging rates are extremely low (CAI et al., 2010). Thus, when ^{228}Th-depleted shelf waters are carried along in the Trans Polar Drift and flow into the low-scavenging regime of the central Arctic, it can be expected that ^{228}Th grows into equilibrium with its parent ^{228}Ra. Here we investigate to what extent the ^{228}Th/^{228}Ra ratio in Arctic surface waters can be used to derive the age of a surface water parcel since it left the high-scavenging regime on the shelf.

2. METHODS

2.1. ARK XI/1 (1995)

During the German-Russian expedition with RV Polarstern to the Laptev Sea, 7 July to 20 Sept. 1995 (RACHOR, 1997), seawater samples of about 40 L were collected at 37 stations (Table 1) with the 24 x 12 L Rosette sampler. After filtration, a solution of barium chloride was added to the samples to coprecipitate radium with $BaSO_4$. At 16 of these stations the samples had previously been acidified, spiked with Fe and ^{230}Th and neutralized with ammonia to isolate Th isotopes on a $Fe(OH)_3$ precipitate. This coprecipitation does not remove Ra (LI et al., 1980). The $BaSO_4$ precipitates were dried and put in small tubes. Radium activities were determined by gamma spectrometry at the home laboratory.

The freshwater components were calculated using the $\delta^{18}O$ data of Frank (1996) and the three-component (Atlantic water, meteoric water and ice melt) mixing model of Östlund and Hut (1984) with endmember compositions according to Ekwurzel et al. (2001).

2.2. ARK XXII/2 (2007)

Surface water samples (150-300L) were collected during Polarstern Expedition ARK XXII/2, 29 July – 7 Oct 2007 (SCHAUER, 2008) (Fig. 1). Samples from the seawater intake at 7m depth were filtered over 1-µm polypropylene cartridges, passed over MnO_2 fibre at a flow rate of at most 1 L/min to obtain a Ra extraction efficiency of at least 97% (MOORE, 2008) and counted for ^{224}Ra with delayed coincidence scintillation counting (MOORE and ARNOLD, 1996). For the calculation of counts due to ^{224}Ra we used the chance coincidence correction,

not the alternative procedure based on total counts (MOORE, 2008). The expected error is 8-14% (GARCIA-SOLSONA et al., 2008). The same procedure can in principle be used to determine ^{227}Ac through ^{223}Ra (GEIBERT et al., 2008) but count rates were influenced by the high count rates of ^{224}Ra and buildup of ^{222}Rn and activities were low and are not reported here. In the home laboratory, Ra was leached from the fibre (ELSINGER et al., 1982), coprecipitated as $BaSO_4$ (CUTTER et al., 2010) and counted with gamma spectroscopy for ^{226}Ra and ^{228}Ra (MOORE, 1984).

Beyond the reach of the unsupported ^{224}Ra from its shelf source (cf. KADKO et al., 2008), ^{224}Ra must be in equilibrium with its parent ^{228}Th. That means that in offshore regions, the delayed coincidence technique provides an indirect technique to monitor ^{228}Th. In studies where excess ^{224}Ra is measured, the ^{224}Ra is recounted after the decay of the first generation ^{224}Ra in order to determine ^{228}Th-supported ^{224}Ra. We have recounted the samples after two half lives and found generally a 20% reduction in count rate. Because we observed this difference even in the central Arctic where an excess activity is not possible at large distance to any potential source, we interpret this not as indication of real in-situ ^{224}Ra excess, but rather as an apparent excess due to insufficient collection of ^{228}Th. This could be due either to filtration, which removes the particulate ^{228}Th, or to non-quantitative adsorption of Th to the Mn fibres. We have also considered the possibility that the seawater inlet of Polarstern had accumulated ^{228}Th during previous expeditions, which would then serve as a continuous source of ^{224}Ra as has been observed on other ships. The fact that we were able to measure low ^{224}Ra in the Atlantic inflow makes it unlikely that such a contamination was a significant contribution to the observed excess ^{224}Ra. We therefore consider the ^{224}Ra activities derived from the initial count rates to represent the total ^{228}Th activity and in this paper will report

them as ^{228}Th. In shelf regions this procedure might overestimate ^{228}Th if a significant contribution of unsupported ^{224}Ra were present. On stations 407 and 411 on the Laptev shelf we deployed in situ pumps and measured ^{228}Th with the double-MnO_2 cartridge technique (BASKARAN et al., 1993) at four horizons. Dissolved ^{228}Th was 13±8 dpm/m^3, particulate ^{228}Th was 1-2 dpm/m^3 compared with a ^{224}Ra activity of 21±15 dpm/m^3 measured with RaDeCC in discrete water samples collected at these stations (Table 2), resulting in an average ^{224}Ra/^{228}Th ratio of 1.45. In five cases where we measured ^{224}Ra (RaDeCC) and ^{228}Th (in situ pumps) at the same station and depth, ^{224}Ra/^{228}Th AR ranged from 0.3-2.1 (Table 2). As values of this AR below 1 are unlikely, we explain the wide range by inhomogeneity while the two isotopes were sampled three hours apart with different gear. We conclude that in individual shelf water samples the measured ^{224}Ra/^{228}Ra may overestimate in situ ^{228}Th/^{228}Ra by up to a factor of 2 (Table 2).

The freshwater and Pacific components for ARK XXII/2 (2007) were calculated using δ^{18}O and nutrient data following (BAUCH et al., 2011) using the N/P characteristics of Atlantic and Pacific waters following Jones et al. (1998) and Yamamoto-Kawai et al. (2008). further details on calculations and errors refer to Bauch et al. (2011). For stations where the calculated Pacific component f_P was negative and for stations on the Laptev shelf (Sta 385 and beyond) f_P was set to zero.

Some depth profiles were obtained on the Laptev shelf with in situ pumps equipped with size-fractionated filters and twin MnO_2-coated cartridges. Cartridges were leached with a Soxhlet system and Ra was precipitated as $BaSO_4$ and gamma counted as the other samples.

The Th fractions of the Soxhlet leaches and of the filter digest solutions (CAI et al., 2010) were analysed for ^{228}Th with alpha spectrometry.

Particulate ^{234}Th was monitored with a semi-automated filtration apparatus (RUTGERS VAN DER LOEFF et al., 2011; RUTGERS VAN DER LOEFF et al., 2006) set to filter approximately every 4 hours 4.9 L of surface water from the ship's seawater intake over 25mm QMA filters that were subsequently dried and counted for beta activity. Graphics were produced with the ODV software package (SCHLITZER, 2010). All data of ^{228}Th and Ra isotopes are presented in Tables 3 and 4 and are available in the database PANGAEA (doi:10.1594/PANGAEA.772682). On this GEOTRACES expedition a wide spectrum of other trace elements and isotopes was measured (see http://www.bodc.ac.uk/geotraces/data/inventories/arkxxii_2/).

3. RESULTS

3.1 ^{226}Ra

In many studies on ^{228}Ra in the open ocean the long-lived isotope ^{226}Ra has been used as a yield tracer determined either in discrete samples (SMITH et al., 2003; RUTGERS VAN DER LOEFF et al., 2003) or derived from published relationships between ^{226}Ra, salinity and silicate (BROECKER et al., 1976; MOORE and SMITH, 1986; RUTGERS VAN DER LOEFF et al., 1995).

A plot of ^{226}Ra activity against f_r (Fig. 2a) shows the major features of ^{226}Ra in surface waters in the Arctic Ocean: First, ^{226}Ra activities in all samples with a significant component of Pacific water are approx 30% higher than in the Eurasian Basin (Fig. 2a and map in Fig. 3). Moore and Smith (1986) had already observed that the surface water concentration of ^{226}Ra at the Cesar Ice camp station (85°50'N, 108°50'W: 107 dpm/m^3) was somewhat higher than reported North Atlantic and Greenland Sea surface values corrected to 35 ‰ salinity and zero dissolved silicate (68-73 dpm/m3, BROECKER et al., 1976); (70±2 to 77±2 for TTO samples N of 70°N KEY et al., 1992). Moore and Smith (1986) argued that the Cesar values were closer to North Pacific surface values from the GEOSECS program (96 dpm/m3 at 32 µM Si, CHUNG and CRAIG, 1980). Similarly high ^{226}Ra activities (113.8, 113.8, 109.7 dpm/m^3) were observed in surface waters of the deep (>1000m) Canada Basin by Smith et al. (2003) but data published for the Chukchi and Beaufort shelf areas (SMITH et al., 2003; KADKO and MUENCH, 2005; LEPORE et al., 2009) are more variable and appear to be strongly affected by biological uptake and release in these productive shelf regions.

Second, offshore surface values in the Eurasian Basin, excluding samples with Pacific influence and samples with significant Ba uptake on the Laptev (Sta 400-411) and Barents (Sta 239) shelves (blue symbols without annotation in figure 2a) have a slight tendency to lower values at higher f_r

$$^{226}Ra = 71.5 - 56\ f_r ; \quad R^2 = 0.33, n=26 \qquad (1)$$

This trend can be compared with data from the Kara Sea (RUTGERS VAN DER LOEFF et al., 2003) that follow the regression $^{226}Ra = 75.2 - 48\ f_r$;$R^2 = 0.91$, n=14, excluding a pure fresh water sample from the Ob river.

229

230 And third, on the Laptev shelf, a prominent effect of biological cycling is observed with
231 ^{226}Ra values in surface waters being reduced by up to 48% relative to eq. 1 (Fig. 2a), while
232 they are enhanced in subsurface waters. A reduction is also observed in the surface water at
233 station 239 (cf. Fe data in Klunder et al., submitted). This biological cycling is closely linked
234 to the cycling of Ba (cf. GUAY and FALKNER, 1997; ABRAHAMSEN et al., 2009; ROESKE et al.,
235 submitted) (Fig. 2b). Both Ba and ^{226}Ra are depleted in the Laptev and Barents (Sta 239)
236 surface waters, while they show enhanced values in Laptev bottom waters. Moreover, both
237 Ba and ^{226}Ra show an offset between Eurasian and Pacific surface waters in the central
238 Basins (cf. ROESKE et al., submitted).
239

240 3.2 ^{228}Ra
241

242 3.2.1 Distribution of ^{228}Ra in summer 2007
243

244 The distribution of ^{228}Ra in 2007 (Fig. 4a) shows high values in the TPD. The surface water
245 in the Atlantic inflow and over the Barents shelf has low ^{228}Ra activities. The maximum
246 activities were found over the Makarov Basin while activities decreased towards the
247 Canadian and Amundsen Basins. For comparison with literature observations we also present
248 the ^{228}Ra data normalized to ^{226}Ra (Fig. 4b). As a result of the Atlantic-Pacific gradient in
249 ^{226}Ra (Fig. 3), the maximum in the ^{228}Ra/^{226}Ra ratio is somewhat shifted towards the
250 Lomonosov Ridge in comparison with the distribution of ^{228}Ra, although this is not easily
251 distinguished in the graphs (Fig. 4b compared to a). Anyhow, the maximum signal in
252 ^{228}Ra/^{226}Ra ratio in the TPD has moved from the Alpha Ridge (SMITH et al., 2003) back

towards the Lomonosov Ridge (Fig. 4b), in agreement with hydrographic observations of this relaxation to anticyclonic, pre-1990s Arctic circulation (MORISON et al., 2006). It should be noted that all samples on the section over the Gakkel Ridge towards the Laptev shelf (section 5) have high ^{228}Ra activities well in excess of the Atlantic inflow, showing the influence of shelf waters. Surface waters on this section have a substantial river water fraction (about 10%), much larger than further west toward Fram Strait at the longitude of the Voronin Trough (on section 3) where ^{228}Ra activities were also much lower.

Bottom waters on the shelf are strongly enriched in ^{226}Ra (Fig. 2b) but also in ^{228}Ra (Fig. 2c). Even higher enrichment of ^{228}Ra in bottom waters of the Chukchi shelf has been observed by Lepore and Moran (2007). Diffusive input of the long-lived ^{226}Ra usually does not cause as prominent an accumulation of ^{226}Ra in shelf waters as is seen for the shorter lived ^{228}Ra. The enrichment of both isotopes in shelf bottom waters therefore implies that the ^{228}Ra accumulation in bottom waters results not only from a release from shelf sediments but also from biological cycling on the shelf. It is not known whether Submarine Groundwater Discharge contributes to this enrichment.

3.2.2 ARK XI/1: defining the freshwater endmember in the Laptev Sea

Intensive sampling in 1995 (ARK XI/1) provides detailed data to define the ^{228}Ra source in the Laptev Sea in that year. ^{226}Ra and ^{228}Ra activities in the Laptev Sea in 1995 are listed in Table 3. Offshore stations have lower ^{228}Ra activities than most shelf stations when plotted against salinity (Fig. 5a). Even if we correct for the dilution by ice melt water by plotting

^{228}Ra against the fraction of river water using δ^{18}O (Fig. 5b), the offshore waters still stand out by their low ^{228}Ra activities. Essentially the same results are obtained when plotting the ^{228}Ra/^{226}Ra activity ratio (AR) (Fig. 5c), implying that the pattern is not a consequence of biological uptake/release. This normalization with ^{226}Ra is justified in the Laptev Sea where the fraction of Pacific water can be neglected. The shelf waters correspond well with earlier data from the Laptev shelf (RUTGERS VAN DER LOEFF et al., 2003). The low offshore ^{228}Ra activities imply either a freshwater source with lower ^{228}Ra activity from the Kara Sea, or the existence of old recirculated water where ^{228}Ra has decayed.

3.3 ^{228}Th/^{228}Ra

^{228}Ra decays to ^{228}Th (1.9 y half life), which in coastal waters is effectively scavenged giving a typical ^{228}Th/^{228}Ra ratio <0.05 in coastal waters (KAUFMAN et al., 1981). Indeed, such low values were also observed in coastal waters of the Canada Basin (TRIMBLE et al., 2004; LEPORE and MORAN, 2007). Further offshore in the Arctic, we know that Th scavenging rates are very low (CAI et al., 2010) which means that ^{228}Th/^{228}Ra ratios must increase by ingrowth.

The ratio of ^{228}Th to its parent ^{228}Ra (Fig. 6) in surface waters over section 3 and section 4+5 across the central Arctic Ocean shows how over the deep basins, the absence of strong scavenging allows ^{228}Th to grow into equilibrium with its parent. The ingrowth of ^{228}Th over the deep basins in contrast to the ^{228}Th-depleted shelf waters is clearly seen in a map of ^{228}Th/^{228}Ra in surface water where the present data are compared with literature values (Fig.

7). Lowest ratios (<0.3) are observed on the Barents, Kara and Laptev shelf and in the Beaufort Sea. Highest ratios (>0.8) are found in the eastern Eurasian Basin including the section over the Gakkel Ridge and on Ice Island T3 in the central Canada Basin. The relatively high AR observed in the low-salinity Polar Surface Layer (PSL) at the ICEX station, only 200km offshore in the Canada Basin, may be explained if this water represents old recirculated water from the Canada Basin (KADKO and MUENCH, 2005). These authors also observed high $^{228}Th/^{228}Ra$ AR on the northern, deep side of their three sections across the Chukchi shelf (their stations 8-18 and 34: depth>500m, AR=0.45±0.08, n=9). All other stations from that study from the shallower waters in Bering Sea and Chukchi shelf had AR≤0.26 (AR:0.09±0.08, n=17). The inflow at the Bering Strait has very low $^{228}Th/^{228}Ra$ AR (<0.06, KADKO and MUENCH, 2005). Lepore and Moran (2007) showed that the wide variation in $^{228}Th/^{228}Ra$ ratios on the Chukchi shelf is in part a seasonal phenomenon.

4. DISCUSSION

4.1 ^{228}Ra

4.1.1 ^{228}Ra vs $^{228}Ra/^{226}Ra$ activity ratio

As mentioned above, the $^{228}Ra/^{226}Ra$ AR has often been used instead of the ^{228}Ra activity itself as tracer. This has the advantage of somewhat better analytical precision because usually ^{228}Ra is calculated from a $^{228}Ra/^{226}Ra$ AR multiplied by the absolute ^{226}Ra activity determined separately. Moreover, the procedure corrects for biological uptake/release. On the

Laptev shelf, biological uptake removed 25-48% of ^{226}Ra and 31% of Ba (ROESKE et al., submitted) in the surface water (Fig. 2). On the other hand, one should always be careful applying a mixing plot using ARs because ratios do not mix linearly (KADKO and MUENCH, 2005) (cf. Fig. 8). Moreover, in the Arctic we see that there are large differences in ^{226}Ra activity between waters from Atlantic and Pacific origin (Fig. 2). In studies like ours with large geographical coverage in the Arctic Ocean, a normalization with ^{226}Ra then requires a correction for the Atlantic/Pacific mixing ratio. For that purpose we introduce here the parameter ^{226}Ra*, in which the ^{226}Ra activity of a sample is corrected for the additional activity it obtained from its Pacific water fraction according to

$$^{226}Ra^{*} = {}^{226}Ra \frac{(f_P + f_A)\ {}^{226}Ra_A}{(f_P\ {}^{226}Ra_P + f_A\ {}^{226}Ra_A)} \qquad (2)$$

where f_A and f_P are the Atlantic and Pacific water fractions and $^{226}Ra_A$ and $^{226}Ra_P$ are the ^{226}Ra activities of pure Atlantic and Pacific waters. In equation (2) the numerator $(f_P + f_A)^{226}Ra_A$ gives the ^{226}Ra if all seawater were of Atlantic origin while the denominator $(f_P{}^{226}Ra_P + f_A{}^{226}Ra_A)$ gives the ^{226}Ra expected from a conservative mixing of the two seawater endmembers. It should be noted that there are few data for the Pacific source water, and that the ^{226}Ra activity for the northernmost Pacific GEOSECS station 219 (96 dpm/m^3 at 20m depth) has a Si concentration of 32µM. If we corrected this for salinity and zero silicate as this was done for Atlantic water by Cochran et al. (1995), we would find an unlikely ^{226}Ra activity in the Pacific source water of only 44±7 dpm/m^3. The value we use here for $^{226}Ra_p$, the average of all samples with a Pacific water component >50% (92.4±1.7 dpm/m^3, n=4, cf. Fig. 2a), should therefore not be regarded as the ^{226}Ra of pure Pacific surface water but of the water that has been preconditioned during its passage through the Bering Strait and over the

neighboring Arctic shelves. This correction procedure introduces further uncertainties. In the following we therefore prefer to discuss ^{228}Ra activities next to ARs.

4.1.2 ^{228}Ra as age marker

The ^{228}Ra distribution (Fig. 4) shows the pathway of the TPD centered over the Makarov Basin with decreasing activities towards the Canada and Amundsen/Nansen Basin. This is consistent with maximum concentrations observed for other tracers of terrigenous influences: Fe (KLUNDER et al., submitted), Mn (MIDDAG et al., 2011), CDOM (Walker and Amon personal communication and Walker 2009). The question we address here is to what extent the deviation from these correlations in the ^{228}Ra data can be interpreted as decay and thus be used as age marker, or rather are due to variability in endmember concentrations. To that effect, we plot the ^{228}Ra activity against the river water component (Fig. 8a). For comparison with literature data where ^{228}Ra has usually been normalized with ^{226}Ra we also show the same data after normalization with ^{226}Ra* in Fig. 8b.

4.1.3 Formation of ^{228}Ra excess on the shelf produces a range of endmembers.

There are two major sources of ^{228}Ra to the ocean: first, by release from sediments, a source that is particularly important on the vast and shallow Siberian shelves. Some further ^{228}Ra may be released from ice rafted sediments upon ice melt. The second major source is a phase adsorbed to riverine particles that is released in the first stages of estuarine mixing. In the Arctic, the first source is considered much more important than the second (Rutgers van der

367 Loeff et al. (2003) and references therein). Although this means that the major source of
368 ^{228}Ra in the Arctic does not coincide with the rivers, it has been argued that the combined
369 effect of the river source and the diffuse shelf source on offshore surface waters (i.e. their
370 "far-field" effect) would be similar to the input of a river component carrying a ^{228}Ra signal.
371 A surface water mass in the central Arctic could then be treated as a mixture of ^{228}Ra-poor
372 seawater, ice-melt water and a freshwater component represented by a virtual endmember
373 ^{228}Ra activity. The early data sets in the central Arctic could be well described by this model,
374 although it was questioned whether the various shelf components could be treated as one
375 single endmember composition (RUTGERS VAN DER LOEFF et al., 1995). In a subsequent
376 paper we found much lower ^{228}Ra activities at the same salinity or river water fraction in the
377 Kara Sea compared to the Laptev Sea, (RUTGERS VAN DER LOEFF et al., 2003). In the Kara
378 Sea the greater depth counteracts the rapid buildup of ^{228}Ra. Schlosser (1994) gives an
379 estimate of 3.5 ± 2 y for residence time of fresh water on Siberian shelves. During this time
380 there is an eastward circulation and shallowing depths from the Kara to the Laptev to the East
381 Siberian Sea before the waters turn northward and leave the shelf in the TPD. It is thus likely
382 that ^{228}Ra continues to accumulate eastward and there is no reason why this further
383 accumulation should be correlated with continued freshwater inputs. This is why we
384 concluded that water may thus reach the shelf edge with variable shelf signatures (RUTGERS
385 VAN DER LOEFF et al., 2003).
386
387 The low ^{228}Ra activities observed offshore in the Laptev Sea during 1995 (Fig. 5) could
388 indeed be interpreted to result from a low-^{228}Ra freshwater source, e.g. from the Barents or
389 Kara Sea. This distribution is confirmed by the data of the 2007 expedition. Surface samples
390 (with $f_r > 2.5\%$) from the Laptev shelf of both expeditions have high ^{228}Ra activities in

391 agreement with the mixing line based on 1991 data from the Eurasian Basin (RUTGERS VAN
392 DER LOEFF et al., 1995). Surface samples of stations with >260m bottom depth of both
393 expeditions have ^{228}Ra activities that are only about half those predicted by the conservative,
394 non-decayed mixing line (Fig. 5c).
395
396 At this point it cannot be decided whether the low offshore ^{228}Ra activities are due to a lower
397 freshwater endmember activity advected from the Kara Sea, or result from decay which
398 would imply that the offshore surface waters contain a river water fraction with a long
399 residence time in the deep Eurasian Basin.
400
401 This situation is very similar to the distribution observed by Kadko and Muench (2005) in the
402 Beaufort Sea. These authors observed much lower ^{228}Ra activities in offshore low salinity
403 Polar Surface Water (Polar Surface Layer, PSL) and concluded that these were waters that
404 had been recirculating in the Canada Basin. They used the ^{228}Ra activities to estimate the age
405 of the PSL water to be up to 14 years. But also in the Canada Basin the actual freshwater
406 ^{228}Ra endmember is not well constrained, and a rigorous distinction between variability in
407 source concentration and radioactive decay cannot be made. In the following we will use the
408 additional tracer ^{228}Th/^{228}Ra to distinguish between these alternative explanations.
409
410 4.2 ^{228}Th/^{228}Ra ratios
411
412 Here we will investigate to what extent the ingrowth of ^{228}Th into the shelf-induced ^{228}Ra can
413 itself serve as a time marker. For this discussion it is essential to know the isotope
414 composition of the water that constitutes the source of the Ra in the central Arctic ocean. In

Fig. 7 we have seen the gradual increase of $^{228}Th/^{228}Ra$ AR from shelf to central ocean, but the differences are even more apparent in a plot of ^{228}Th versus ^{228}Ra (Fig. 9). There is a large variation in concentrations on the shelves and part of the variation in $^{228}Th/^{228}Ra$ AR is seasonal (LEPORE and MORAN, 2007). While plankton growth and export leads to the removal of thorium, there is also a significant uptake of radium (Fig. 2), which might even contribute to the sometimes relatively high AR values in shelf waters with low ^{228}Ra (Fig. 9). However, these ^{228}Ra-depleted shelf waters clearly cannot be the source of the high ^{228}Ra activities in the TPD (51-92 dpm m^{-3} and one exceptionally high value of 123 dpm m^{-3}, Sta 349). Instead we must look for source waters with at least a similarly high ^{228}Ra activity. At high ^{228}Ra activities (>80 dpm m^{-3}) the $^{228}Th/^{228}Ra$ AR is only 0.1-0.2 (Fig. 9) and in the following we will assume that the ^{228}Ra-enriched shelf water leaves the shelf with an AR $F_0=0.15\pm0.05$. As we will show later, the age estimates are not very sensitive to errors in F_0.

4.3 Models for the distribution of ^{228}Ra and ^{228}Th.

4.3.1 constant ^{228}Ra: concordia with $^{234}Th/^{238}U$.

In a system with a constant ^{228}Ra (and ^{238}U) activity and a constant scavenging rate of Th, the steady state $^{228}Th/^{228}Ra$ values should be concordant with $^{234}Th/^{238}U$ ratios (KAUFMAN et al., 1981). Indeed, the range of values we observed on the shelf is concordant with observed $^{234}Th/^{238}U$ ratios of 0.8-0.9 (CAI et al., 2010) (Fig. 10a).

A similar calculation can be made for the deep basins. Here, the very low thorium scavenging rates found by Cai et al. (2010) must allow ^{228}Th activities to increase. Outside

439 the more productive shelf regions the depletion of ^{234}Th with respect to ^{238}U was largely
440 limited to the upper mixed layer which was usually only approx 20m deep. In 30 stations
441 over the slope and the central basin ^{234}Th/^{238}U in the surface layer (5m depth) was 0.89 ±
442 0.11. But the depletion follows a distinct geographical trend (Fig. 11, data from CAI et al.,
443 2010). The five stations on the Barents slope (depth range 1533-3115m) stand out by strong
444 depletion (^{234}Th/^{238}U <0.8) (Fig. 11b) which we attribute to export related with production
445 influenced by the Barents shelf (WASSMANN et al., 1999; WASSMANN et al., 2004; LALANDE
446 et al., 2008), as was also observed in Ba (ROESKE et al., submitted) and Fe (KLUNDER et al.,
447 submitted) data. Excluding the Barents slope, the average ^{234}Th/^{238}U in the surface layer of
448 all stations with depth >1500m was 0.942 ± 0.060 (n=18) in good agreement with the data
449 from three permanently ice-covered stations in the Canada Basin sampled by Trimble and
450 Baskaran (2005) (0.946 ± 0.057). If we restrict the region further to the central Arctic N of
451 84°35'N the average becomes 0.958 ± 0.058 (n=11). These ^{234}Th/^{238}U ratios correspond in
452 steady state to a thorium scavenging rate of 0.46 (0-1.16) y^{-1}. Again in steady state, this
453 would cause a ^{228}Th/^{228}Ra ratio of 0.24-1.0. Indeed, in the central Eurasian and Canada
454 basins ^{228}Th/^{228}Ra ratios (our own and literature values) are far above the ratio of shelf waters
455 (Figs 6, 7, 9). But apart from the crude comparison in Fig. 10, the concordia concept is not a
456 satisfactory description of the data. The isotope distribution cannot be described as steady
457 state because, as we shall see, ingrowth of ^{228}Th causes gradual changes in the ^{228}Th/^{228}Ra
458 ratio. Seasonal variations are a further cause of large deviations from concordia, especially in
459 shelf areas (LEPORE and MORAN, 2007).
460
461 4.3.2 open system approach: eddy diffusion.

462

463 In ocean margins where ^{228}Ra is released from coastal sediments and where coastal waters
464 exchange with offshore waters by horizontal mixing (eddy diffusion), ^{228}Ra decreases
465 exponentially with distance offshore by horizontal mixing and decay. In these systems the
466 distribution of ^{228}Th (activity A_T) is governed by decay of ^{228}Ra (activity A_R), ingrowth and
467 scavenging of ^{228}Th (scavenging rate λ_s) and mixing, as discussed by Broecker et al. (1973):

468 $$\lambda_R A_R = k \frac{\partial^2 A_R}{\partial x^2} \quad (3)$$

469 $$(\lambda_T + \lambda_s) A_T = A_R \lambda_T + k \frac{\partial^2 A_T}{\partial x^2} \quad (4)$$

470 where k is the horizontal eddy diffusion coefficient, x is distance offshore and λ_R and λ_T are
471 the decay constants of ^{228}Ra and ^{228}Th, respectively. The offshore distribution of ^{228}Ra
472 follows a simple exponential decay (BROECKER et al., 1973):

473 $$A_R = A_{R^0} e^{-\sqrt{\frac{\lambda_R}{k}} x} \quad (5)$$

474 where the superscript ° denotes the situation when the water leaves the shelf. For the
475 boundary condition of a constant ^{228}Th/^{228}Ra AR on the shelf (F_0) we find the solution:

476 $$A_T = \frac{\lambda_T A_{R^0}}{\lambda_T + \lambda_s - \lambda_R} e^{-\sqrt{\frac{\lambda_R}{k}} x} + (F_0 A_{R^0} - \frac{\lambda_T A_{R^0}}{\lambda_T + \lambda_s - \lambda_R}) e^{-\sqrt{\frac{\lambda_T + \lambda_s}{k}} x} \quad (6)$$

477 which for the condition of 100% scavenging on the shelf (F_0=0) simplifies to (BROECKER et
478 al., 1973)

479 $$A_T = \frac{\lambda_T A_{R^0}}{\lambda_T + \lambda_s - \lambda_R} (e^{-\sqrt{\frac{\lambda_R}{k}} x} - e^{-\sqrt{\frac{\lambda_T + \lambda_s}{k}} x}) \quad (7)$$

480 Equations (5) and (6) define a relationship between ^{228}Th and ^{228}Ra,

481 $$A_T = \frac{\lambda_T}{\lambda_T + \lambda_s - \lambda_R} A_R + (F_0 - \frac{\lambda_T}{\lambda_T + \lambda_s - \lambda_R}) A_{R^0} \left(\frac{A_R}{A_{R^0}} \right)^{\sqrt{\frac{\lambda_T + \lambda_s}{\lambda_R}}} \quad (8)$$

482 which is displayed in Fig. 12 for several values of the Th scavenging rate and a shelf source
483 with a ^{228}Th/^{228}Ra AR F_0=0.15. We have already seen that the ^{228}Ra activity of this source is
484 not well constrained. Based on the distribution of concentrations in shelf waters we use here
485 110 dpm m^{-3} although locally activities up to 180 dpm m^{-3} are found (Table 3), and even
486 higher in bottom waters on the shelves. With these assumptions, the mixing model cannot
487 explain our data. This conclusion is not affected by possible changes in F_0 (broken lines in
488 Fig. 12) as might e.g result from our overestimate of ^{228}Th on the shelf due to excess ^{224}Ra.
489 Especially for the high ^{228}Ra activities we observed in the TPD, the high ^{228}Th data are
490 incompatible with the mixing model, even in the absence of scavenging (λ_s=0). The
491 continued exchange in this model with the Th-depleted shelf water does not allow Th to grow
492 to the high values observed offshore.
493
494 4.3.3 closed system approach: advection
495
496 Neither the steady state model with constant ^{228}Ra and ^{238}U activities leading to a concordia
497 with ^{234}Th/^{238}U, nor a mixing model based on eddy diffusion gives an appropriate
498 representation of the situation in the central Arctic. Here the surface circulation is
499 characterized by the TPD. When the shelf waters turn offshore, lose contact with the shelf
500 and flow as a thin lens over deep water, ^{228}Ra is no longer supplied by the sediments and will
501 decay. At the same time, the reduction in scavenging rate will allow the gradual ingrowth of
502 ^{228}Th. In this advective system it is more appropriate to calculate the time development of

503 parent and daughter as the net result of decay of ^{228}Ra, ingrowth of ^{228}Th and removal of
504 ^{228}Th by scavenging, but without horizontal mixing. If we assume that the scavenging is
505 reduced to a low open ocean value as soon as the water mass leaves contact with the shelf,
506 the ingrowth of ^{228}Th will follow the two-decay curve:

507 $$A_T = A_{T^0} e^{-(\lambda_T + \lambda_s)t} + \frac{\lambda_T + \lambda_s}{\lambda_T + \lambda_s - \lambda_R} A_{R^0} (e^{-\lambda_R t} - e^{-(\lambda_T + \lambda_s)t}) \quad (9)$$

508 where the superscript ° again denotes the situation a t=0 when the water leaves the shelf. This
509 model does not include mixing. There is a strong vertical gradient in ^{228}Ra activity in the
510 halocline (RUTGERS VAN DER LOEFF et al., 1995). Although stratification is strong, mixing
511 will cause some loss of ^{228}Ra to deeper waters. As the ^{228}Th gradient is in the same direction,
512 the ratio should not be strongly affected by this loss by mixing.
513
514 In Fig. 13 the evolution of ^{228}Th and of the ^{228}Th/^{228}Ra AR has been modeled for several
515 values of λ_s. Note that the evolution of the AR in this model is independent on the actual
516 value of ^{228}Ra in the shelf source. An error in the value used for F_0 causes a relatively small
517 error in the predicted ages. If for example a water parcel leaves the shelf with an F_0 of 0.1, it
518 would take just 2-3 months for the ingrowth to reach the value of 0.15, the starting point of
519 our model calculations.
520 The model results show that many observed ^{228}Th/^{228}Ra ratios in the central Arctic Ocean
521 (Fig. 7) can never be reached with the ^{234}Th-based average scavenging rate of 0.46 y^{-1}. The
522 observed ^{228}Th/^{228}Ra ratio of 0.8 sets an upper limit to λ_s of 0.21 y^{-1}. This can be explained
523 when the scavenging rate over the longer time horizon recorded by ^{228}Th is lower than the
524 recent summer value recorded by the short lived ^{234}Th. Based on the ingrowth model, we can
525 now derive an age since the water mass detached from the shelf area. In a first

526 approximation, we assume that $\lambda_s = 0.21\ y^{-1}$ throughout the deep Arctic Ocean and determine
527 the age based on the $^{228}Th/^{228}Ra$ ingrowth using equation 9. The results (Fig. 14) confirm the
528 high age of the fresh water component observed in the central Eurasian Basin over the
529 Gakkel Ridge. Even in the absence of scavenging, ingrowth to the AR values observed at
530 stations 371-382 (0.90 ± 0.10 to 1.24 ± 0.13) requires 2.7-4.1 to >5.2y, respectively. This is
531 a strong argument that the low ^{228}Ra values observed offshore in the Laptev Sea in 1995 and
532 2007 (Fig. 5c) are due to decay during recirculation of these waters and not to an input of
533 low-radium water from the Kara Sea.
534
535 In the age calculation above we have assumed that once the water has left the shelves, the
536 scavenging rate is everywhere the same. The high $^{228}Th/^{228}Ra$ ratios in the Nansen Basin of
537 0.8 require an ingrowth period of at least 3 years even if no scavenging had occurred. But the
538 reduced $^{228}Th/^{228}Ra$ ratios over the Lomonosov Ridge and over the southern part of the
539 Gakkel Ridge could be explained either by a rapid transport from the shelf or by a somewhat
540 higher scavenging rate. We have therefore looked for indications of spatial differences in
541 suspended particulate material and scavenging rates.
542
543 4.4 Evidence for regional differences in scavenging rates
544
545 4.4.1 Transmissometry
546
547 The clearest waters, as deduced from transmissometer readings (Fig. 15) were found over the
548 Nansen Basin and in the Makarov/Alpha Ridge region. Light transmission was reduced over

549 the Amundsen Basin and Lomonosov Ridge and over most of section 5 over the Gakkel
550 Ridge towards the Laptev shelf.
551
552 4.4.2 Particulate ^{234}Th
553
554 Particulate ^{234}Th in surface water can be considered as a proxy for the suspended matter load
555 (RUTGERS VAN DER LOEFF et al., 2011). Indeed, the distribution of particulate ^{234}Th (Fig. 16)
556 resembles well the distribution of light transmission, with the same features: relatively high
557 values during passing of the Lomonosov Ridge, especially during the first section (3). On the
558 second section (4) we observed again enhanced values, then especially on the Amundsen side
559 of the Lomonosov Ridge. We found enhanced values also over most of section 5 over the
560 Gakkel Ridge towards the Laptev Sea and slightly enhanced values over the Alpha Ridge.
561 The lowest values, corresponding to the clearest water, were found in the Nansen Basin, the
562 Siberian side of the Amundsen Basin and the southern part of the Makarov Basin. The large
563 differences between the two sections over the Makarov Basin point at temporal changes in
564 the composition of the TPD. Bauch et al. (BAUCH et al., 2011) came to a similar conclusion
565 based on δ^{18}O data from these sections.
566
567 4.4.3 Total ^{234}Th/^{238}U: export from surface layer
568
569 In the far offshore region with latitude >84°35' we had found from the data of Cai et al.
570 (2010) an average ^{234}Th/^{238}U ratio of 0.958 ± 0.058 (n=11). The nine stations with depth
571 >1500m (depth >1500m, lat>84°35') have ^{234}Th/^{238}U = 0.975 ± 0.047 (n=9). The two
572 stations close the Lomonosov Ridge stand out with ^{234}Th/^{238}U values of 0.90 ± 0.04 (Sta 316,

573 1298m bottom depth) and 0.86 ± 0.04 (Sta 358, 1424m). The $^{234}Th/^{238}U$ ratio of 0.90
574 observed over the Lomonosov Ridge (station 316, August 30: 0.90 ± 0.04; station 358, Sept
575 11: 0.86 ± 0.04.) corresponds in steady state with a scavenging rate of 1.17 y^{-1}.
576
577 With this scavenging rate, the $^{228}Th/^{228}Ra$ AR could not have increased above 0.26 (Fig.
578 13b). As we observed a ratio of 0.5, we again conclude that the scavenging must have been
579 seasonally increased. The Th scavenging rate observed from $^{234}Th/^{238}U$ disequilibrium in
580 summer 2007 may thus represent a maximum over a year as primary productivity is typical at
581 its highest in this season. Also, particle export studies using sediment traps indicate that POC
582 export is at its highest in summer (CAI et al., 2010) (and references therein). Therefore, there
583 is a good reason to use for λ_s a lower year-round average value than the one calculated using
584 summer ^{234}Th data. A short summer increase in λ_s would also affect ^{228}Th activities, but the
585 relative effect would be smaller for the longer lived ^{228}Th, which would already be depleted
586 by about 50% before the summer, than for the short-lived ^{234}Th, with a depletion of only
587 10%.
588
589 The combined evidence (Fig. 17) infers an enhanced particle load and scavenging rate in the
590 area of the Lomonosov Ridge. Apparently, the shelf input in this region is so large that even
591 this far offshore it enhances productivity and export above the neighboring regions. It is also
592 likely that the increased particle load and scavenging rate is related to the release of ice-
593 rafted particles upon ice melt (BASKARAN et al., 2003; TRIMBLE and BASKARAN, 2005).
594
595 4.5 Synthesis/comparison of the models

In Fig. 18 we compare our and selected literature data of ^{228}Th and ^{228}Ra in surface waters of the offshore Arctic Ocean with the predictions of the various models discussed. All stations are sufficiently far offshore that excess ^{224}Ra must have decayed and the measured ^{224}Ra is a good proxy for ^{228}Th. The observations in the TPD, especially all samples with ^{228}Ra>75 dpm m^{-3} (stations 322-352 or all stations on the Canadian side of the Lomonosov Ridge, Cesar station) are incompatible with the mixing model at any value of λ_s and best explained by the advective model. The values over the Lomonosov Ridge are also incompatible with the mixing model if we realize that scavenging cannot be disregarded here. Based on the ^{228}Th/^{228}Ra ingrowth in the advective model (Fig. 13), the minimum shelf water age of surface waters (disregarding scavenging) in the TPD ranges from 1.2 yr near the Lomonosov Ridge (AR=0.49) to 2.7 y in the Makarov Basin/Alpha Ridge (AR=0.79). With the evidence of enhanced scavenging rates over the Lomonosov Ridge it is more likely that the age of water over that Ridge is rather $\geq$ 3 yr.

The interpretation of the data in the Eurasian basin is more difficult because the ^{228}Ra activities are much lower and for these activities the model results tend to approach each other. Nevertheless, the high AR for the samples over the northern part of the Gakkel Ridge require time to accumulate. In the advective model, the AR of 0.9 and above would not be reached before 3.4 years, even disregarding scavenging. The ^{228}Th accumulation over the Gakkel Ridge shows that the surface water cannot flow here in parallel to the TPD with the rate experienced for the ice by the Tara drift. It is more likely that a recirculating gyre exists, increasing the residence time of the surface water in the Eurasian Basin.

5. CONCLUSIONS

Similar to Ba, Ra is clearly affected by biological uptake in surface waters of the Arctic shelves and release in their bottom waters. The biological effect on ^{228}Ra distribution can be corrected for by normalizing with ^{226}Ra. But ^{226}Ra also resembles Ba in enhanced concentrations in waters of Pacific origin compared to waters of Atlantic origin. This difference has to be accounted for when ^{228}Ra/^{226}Ra ratios are used in pan Arctic studies.

In the central Arctic, ^{228}Ra is at its maximum over the Lomonosov Ridge and Makarov Basin. If the maximum has moved towards the Canada Basin in the early nineties (SMITH et al., 2003), it has moved back with the change to more anticyclonic surface water circulation (MORISON et al., 2006).

The half life of ^{228}Ra (5.8 y) is appropriate for the study of shelf water transport in the TPD. But the use of ^{228}Ra as age marker for shelf waters requires that the shelf source of ^{228}Ra is constant in space and time. Judged from the transit times of ice (1.5-4y) and surface water (minimum estimate 2-5y, SCHLOSSER et al., 1999) the initial ^{228}Ra must be known to clearly better than 50%. We cannot judge whether this condition is met to a sufficient extent to allow the calculation of ages with acceptable error limits for the relatively rapid transport in the TPD.

642 Seasonal removal of Th and Ra produces a wide range of ^{228}Ra activities and ^{228}Th/^{228}Ra
643 ratios on the shelves. The high ^{228}Ra activities in the central Arctic Ocean imply that these
644 Ra-depleted shelf waters cannot be the source for the TPD. Shelf waters with sufficiently
645 high ^{228}Ra activity (>100 dpm m^{-3}) usually have low ^{228}Th/^{228}Ra (AR<0.2), and we assume
646 that these waters leave the shelf with a ^{228}Th/^{228}Ra activity ratio (F_0) of 0.15 ± 0.10.
647 ^{228}Th/^{228}Ra ratios in surface waters increase through 0.4-0.6 in the TPD over the Lomonosov
648 Ridge to 0.8-1.0 over the deep basins. The ingrowth of ^{228}Th into its ^{228}Ra parent thus
649 provides independent age information of surface waters. However, the interpretation of this
650 information with an ingrowth-scavenging model is complicated by clear geographical
651 differences in scavenging rates. Transmission, particulate ^{234}Th, and ^{234}Th/^{238}U data
652 consistently show enhanced suspended particulate matter concentrations and correspondingly
653 high scavenging rates over the Lomonosov Ridge compared to the adjacent deep basins.
654
655 The minimum shelf water age of surface water over the Lomonosov Ridge, estimated with
656 neglect of scavenging, is 1.1 yr. With the evidence of enhanced scavenging rates over the
657 Lomonosov Ridge it is more likely that the age of water over that Ridge is rather ≥3 yr. The
658 surface water on the Canadian side of the TPD is older as has been shown in previous studies
659 (RUTGERS VAN DER LOEFF et al., 1995; HANSELL et al., 2004; LETSCHER et al., 2011).
660 Similarly, the minimum age of fresh water over the Gakkel Ridge is 3.4 yr, but with realistic
661 scavenging rates this must be appreciably longer. ^{228}Ra distribution and ^{228}Th/^{228}Ra ingrowth
662 give independent proof of the high age of the water in the eastern Eurasian basin over the
663 Gakkel Ridge. We conclude that there must be a recirculation of shelf water in this basin
664 (Fig. 19), as this has been suggested in earlier studies of surface circulation (GORDIENKO and

665 LAKTIONOV, 1969). This situation is very similar to the inferred recirculation of shelf water
666 in the Canada Basin near the ICEX station (KADKO and MUENCH, 2005).
667
668 **ACKNOWLEDGMENTS**
669
670 We wish to thank the captain and crew of RV Polarstern during the expeditions ARK XI/1
671 (1995) and ARK XXII/2 (2007). Sampling and analysis in 1995 was done by Françoise
672 Legeleux. We thank the chief scientists Eike Rachor and Ursula Schauer for their part in
673 organizing the expeditions, the oceanography teams of both expeditions for their help in
674 collecting samples and providing data for T,S and light transmission, and Karel Bakker for
675 nutrient analyses during ARK XXII/2. We are grateful for help in mathematics from Dieter
676 Wolf Gladrow, for discussions with Bert Rudels, Michael Karcher and Jean Louis Reyss and
677 for constructive reviews by Mark Baskaran, David Kadko and an anonymous reviewer. TR
678 was funded by the EU Sixth Framework Programme DAMOCLES (Developing Arctic
679 Modelling and Observing Capabilities for Long-term Environment Studies), contract number
680 018509GOCE. SBM acknowledges support from NSF award OPP-0124917.
681
682
683
684

685 **REFERENCES**
686
687 Abrahamsen, E. P., Meredith, M. P., Falkner, K. K., Torres-Valdes, S., Leng, M. J., Alkire,
688 M. B., Bacon, S., Laxon, S., Polyakov, I., and Ivanov, V., 2009. Tracer-derived
689 freshwater composition of the Siberian continental shelf and slope following the
690 extreme Arctic summer of 2007. *Journal of Geophysical Research* **36**, L07602,
691 doi:10.1029/2009GL037341.
692 Bacon, M. P., Huh, C.-A., and Moore, R. M., 1989. Vertical profiles of some natural
693 radionuclides over the Alpha Ridge, Arctic Ocean. *Earth Planet. Sci. Lett.* **95**, 15-22.
694 Baskaran, M., Murphy, D. J., Santschi, P. H., Orr, J. C., and Schink, D. R., 1993. A method
695 for rapid in situ extraction and laboratory determination of Th, Pb, Ra isotopes from
696 large volumes of seawater. *Deep-Sea Res.* **40**, 849-865.
697 Baskaran, M., Swarzenski, P. W., and Porcelli, D., 2003. Role of colloidal material in the
698 removal of ^{234}Th in the Canada basin of the Arctic Ocean. *Deep Sea Research Part I:*
699 *Oceanographic Research Papers* **50**, 1353-1373.
700 Bauch, D., Rutgers van der Loeff, M., Andersen, N., Bakker, K., Torres-Valdes, S., and
701 Abrahamsen, P., 2011. Origin of freshwater and polynya water in the Arctic Ocean
702 halocline in 2007. *Prog. Oceanogr.* **91**, 482-495.
703 Broecker, W. S., Goddard, J., and Sarmiento, J. L., 1976. The distribution of ^{226}Ra in the
704 Atlantic Ocean. *Earth Planet. Sci. Lett.* **32**, 220-235.
705 Broecker, W. S., Kaufman, A., and Trier, R. M., 1973. The residence time of Thorium in
706 surface seawater and its implications regarding the fate of reactive pollutants. *Earth*
707 *Planet. Sci. Lett.* **20**, 35-44.
708 Cai, P., Rutgers v.d. Loeff, M. M., Stimac, I., Nöthig, E.-M., Lepore, K., and Moran, S. B.,
709 2010. Low export flux of particulate organic carbon in the central Arctic Ocean as
710 revealed by ^{234}Th:^{238}U disequilibrium. *Journal of Geophysical Research - Oceans*
711 **115**, C10037, doi:10.1029/2009JC005595.
712 Chung, Y. and Craig, H., 1980. ^{226}Ra in the Pacific Ocean. *Earth and Planetary Science*
713 *Letters* **49**, 267-292.
714 Cochran, J. K., Hirschberg, D. J., Livingston, H. D., Buesseler, K. O., and Key, R. M., 1995.
715 Natural and anthropogenic radionuclide distributions in the Nansen Basin, Arctic
716 Ocean: Scavenging rates and circulation time scales. *Deep-Sea Res. II* **42**, 1495-1517.
717 Coppola, L., Roy-Barman, M., Wassmann, P., Mulsow, S., and Jeandel, C., 2002. Calibration
718 of sediment traps and particulate organic carbon using ^{234}Th in the Barents Sea. *Mar.*
719 *Chem.* **80**, 11-26.
720 Cutter, G., Andersson, P., Codispoti, L., Croot, P., Francois, R., Lohan, M., Obata, H., and
721 Loeff, M. R. v. d., 2010. Sampling and Sample-handling Protocols for GEOTRACES
722 Cruises. In: www.geotraces.org (Ed.).
723 Ekwurzel, B., Schlosser, P., Mortlock, R. A., Fairbanks, R. G., and Swift, J. H., 2001. River
724 runoff, sea ice meltwater, and Pacific water distribution and mean residence times in
725 the Arctic Ocean. *J. Geophys. Res.* **106**, 9075-9092.
726 Elsinger, R. J., King, P. T., and Moore, W. S., 1982. Radium-224 in natural waters measured
727 by g ray spectrometry. *Anal. Chim. Acta* **144**, 277-281.
728 Frank, M., 1996. Spurenstoffuntersuchungen zur Zirkulation im eurasischen Becken des
729 Nordpolarmeeres. Ph.D., Ruprecht Karls Univ.

730 Garcia-Solsona, E., Garcia-Orellana, J., Masqué, P., and Dulaiova, H., 2008. Uncertainties
731 associated with 223Ra and 224Ra measurements in water via a Delayed Coincidence
732 Counter (RaDeCC). *Marine Chemistry* **109**, 198.
733 Geibert, W., Charette, M., Kim, G., Moore, W. S., Street, J., Young, M., and Paytan, A.,
734 2008. The release of dissolved actinium to the ocean: A global comparison of
735 different end-members. *Marine Chemistry* **109**, 409.
736 Gordienko, P. A. and Laktionov, A. F., 1969. Circulation and physics of the Arctic Basin
737 Waters. In: Gordon, A. and Baker, F. W. G. (Eds.), *Annals of the the International*
738 *Geophysical Year, Oceanography*. Pergamon, New York.
739 Guay, C. K. and Falkner, K. K., 1997. Barium as a tracer of Arctic halocline and river waters.
740 *Deep-Sea Res. II* **44**, 1543-1569.
741 Hansell, D. A., Kadko, D., and Bates, N. R., 2004. Degradation of Terrigenous Dissolved
742 Organic Carbon in the Western Arctic Ocean. *Science* **304**, 858-861.
743 Jones, E. P., Anderson, L. G., and Swift, J. H., 1998. Distribution of Atlantic and Pacific
744 waters in the upper Arctic Ocean: Implications for curculation. *Geophys. Res. Lett.*
745 **25**, 765-768.
746 Kadko, D. and Aagaard, K., 2009. Glimpses of Arctic Ocean shelf–basin interaction from
747 submarine-borne radium sampling. *Deep-Sea Research I* **56**, 32-40.
748 Kadko, D. and Muench, R., 2005. Evaluation of shelf-basin interaction in the western Arctic
749 by use of short-lived radium isotopes: The importance of mesoscale processes. *Deep*
750 *Sea Research Part II: Topical Studies in Oceanography* **52**, 3227.
751 Kadko, D., Pickart, R. S., and Mathis, J., 2008. Age characteristics of a shelf-break eddy in
752 the western Arctic and implications for shelf-basin exchange. *Journal of Geophysical*
753 *Research* **113**, doi:10.1029/2007JC004429.
754 Kaufman, A., Li, Y.-H., and Turekian, K. K., 1981. The removal rates of ^{234}Th and ^{228}Th
755 from waters of the New York Bight. *Earth and Planetary Science Letters* **54**, 385-
756 392.
757 Key, R. M., Moore, W. S., and Sarmiento, J. L., 1992. *Transient Tracers in the Ocean North*
758 *Atlantic Study. Final Data Report for ^{228}Ra and ^{226}Ra.* Ocean Tracer Laboratory,
759 Princeton, NJ, USA, 193 pp.
760 Klunder, M. B., Bauch, D., Laan, P., Baar, H. J. W. D., Heuven, S. v., and Ober, S.,
761 submitted. Dissolved iron in the Arctic shelf seas and surface waters of the Central 1
762 Arctic Ocean: Impact of Arctic river water and ice-melt. *Journal of Geophysical*
763 *Research - Oceans*.
764 Lalande, C., Lepore, K., Cooper, L. W., Grebmeier, J. M., and Moran, S. B., 2007. Export
765 fluxes of particulate organic carbon in the Chukchi Sea: A comparative study using
766 ^{234}Th/^{238}U disequilibria and drifting sediment traps *Mar. Chem.* **103**, 185–196.
767 Lalande, C., Moran, S. B., Wassmann, P., Grebmeier, J. M., and Cooper, L. W., 2008. ^{234}Th-
768 derived particulate organic carbon fluxes in the northern Barents Sea with comparison
769 to drifting sediment trap fluxes. *Journal of Marine Systems* **73**, 103.
770 Lepore, K. and Moran, B., 2007. Seasonal changes in thorium scavenging and particle
771 aggregation in the western Arctic Ocean. *Deep-Sea Research I* **54**, 919-938.
772 Lepore, K., Moran, S. B., Grebmeier, J. M., Cooper, L. W., Lalande, C., Maslowski, W.,
773 Hill, V., Bates, N. R., Hansell, D. A., Mathis, J. T., and Kelly, R. P., 2007. Seasonal
774 and interannual changes in particulate organic carbon export and deposition in the
775 Chukchi Sea. *J. Geophys. Res.* **112**.

776 Lepore, K., Moran, S. B., and Smith, J. N., 2009. 210Pb as a tracer of shelf-basin transport
777 and sediment focusing in the Chukchi Sea. *Deep Sea Research Part II: Topical*
778 *Studies in Oceanography* **56**, 1305-1315.
779 Letscher, R. T., Hansell, D. A., and Kadko, D., 2011. Rapid removal of terrigenous dissolved
780 organic carbon over the Eurasian shelves of the Arctic Ocean. *Marine Chemistry* **123**,
781 78-87.
782 Li, Y.-H., Feely, H. W., and Toggweiler, J. R., 1980. ^{228}Ra and ^{228}Th concentrations in
783 GEOSECS Atlantic surface waters. *Deep-Sea Res.* **27A**, 545-555.
784 McLaughlin, F. A., Carmack, E. C., Macdonald, R. W., and Bishop, J. K. B., 1996. Physical
785 and geochemical properties across the Atlantic/Pacific water mass front in the
786 southern Canadian Basin. *Journal of Geophysical Research* **101**, 1183-1197.
787 Middag, R., de Baar, H. J. W., Laan, P., and Klunder, M. B., 2011. Fluvial and hydrothermal
788 input of manganese into the Arctic Ocean. *Geochimica et Cosmochimica Acta* **75**,
789 2393-2408.
790 Moore, R. M. and Smith, J. N., 1986. Disequilibria between ^{226}Ra, ^{210}Pb and ^{210}Po in the
791 Arctic Ocean and the implications for the chemical modification of the Pacific water
792 inflow. *Earth Planet. Sci. Lett.* **77**, 285-292.
793 Moore, W. S., 1984. Radium isotope measurements using germanium detectors. *Nuclear*
794 *Instruments and Methods in Physics Research* **223**, 407-411.
795 Moore, W. S., 2008. Fifteen years experience in measuring ^{224}Ra and ^{223}Ra by delayed
796 coincidence counting. *Mar. Chem.* **109**, 188.
797 Moore, W. S. and Arnold, R., 1996. Measurement of ^{223}Ra and ^{224}Ra in coastal waters using
798 a delayed coincidence counter. *J. Geophys. Res.* **101**, 1321-1329.
799 Moore, W. S., Sarmiento, J. L., and Key, R. M., 1986. Tracing the Amazon component of
800 surface Atlantic water using ^{228}Ra, salinity and silica. *J. Geophys. Res.* **91**, 2574-
801 2580.
802 Moran, S. B., Ellis, K. M., and Smith, J. N., 1997. ^{234}Th/^{238}U disequilibrium in the central
803 Arctic Ocean: implications for particulate organic carbon export. *Deep-Sea Res. II* **44**,
804 1593-1606.
805 Moran, S. B., Kelly, R. P., Hagstrom, K., Smith, J. N., Grebmeier, J. M., Cooper, L. W.,
806 Cota, G. F., Walsh, J. J., Bates, N. R., Hansell, D. A., Maslowski, W., Nelson, R. P.,
807 and Mulsow, S., 2005. Seasonal changes in POC export flux in the Chukchi Sea and
808 implications for water column-benthic coupling in Arctic shelves. *Deep-Sea Research*
809 *II* **52**, 3427–3451.
810 Moran, S. B. and Smith, J. N., 2000. ^{234}Th as a tracer of scavenging and particle export in the
811 Beaufort Sea. *Cont. Shelf Res.* **20**, 153-167.
812 Morison, J., Steele, M., Kikuchi, T., Falkner, K., and Smethie, W., 2006. Relaxation of
813 central Arctic Ocean hydrography to pre-1990s. *Geophys. Res. Letters* **33**.
814 Östlund, G. and Hut, G., 1984. Arctic Ocean water mass balance from isotope data. *J.*
815 *Geophys. Res.* **89**, 6373-6381.
816 Pfirman, S., Tremblay, B., and Fowler, C., 2009. Going with the Floe? *American Scientist*
817 **97**, 484-493.
818 Pfirman, S. L., Colony, R., Nürnberg, D., Eicken, H., and Rigor, I., 1997. Reconstructing the
819 origin and trajectory of drifting Arctic sea ice. *Journal of Geophysical Research* **102**,
820 12575-12586.

Proshutinsky, A. Y. and Johnson, M. A., 1997. Two circulation regimes of the wind-driven Arctic Ocean. *Journal of Geophysical Research* **102**, 12,493-12,514, doi:10.1029/97JC00738.

Rachor, E., 1997. Scientific Cruise Report of the Arctic Expedition ARK-XI/1 of RV "Polarstern" in 1995. *Reports on Polar and Marine Research* **226**, 156pp, 6 annexes.

Roeske, T., Bauch, D., and Rutgers v. d. Loeff, M., submitted. Utility of dissolved Barium in distinguishing North American from Eurasian runoff in the Arctic Ocean. *Marine Chemistry*.

Rudels, B., 2009. Ocean Current: Arctic Basin Circulation. In: Steele, J., Thorpe, S., and Turekian, K. (Eds.), *Encyclopedia of Ocean Sciences*. Academic Press.

Rutgers van der Loeff, M. M., Cai, P., Stimac, I., Bracher, A., Middag, R., Klunder, M., and Van Heuven, S., 2011. ^{234}Th in surface waters: distribution of particle export flux across the Antarctic Circumpolar Current and in the Weddell Sea during the GEOTRACES expedition ZERO and DRAKE, . *Deep Sea Research II.* **58**, 2749-2766, doi:10.1016/j.dsr2.2011.02.004.

Rutgers van der Loeff, M., Kuhne, S., Wahsner, M., Holtzen, H., Frank, M., Ekwurzel, B., Mensch, M., and Rachold, V., 2003. ^{228}Ra and ^{226}Ra in the Kara and Laptev seas. *Cont. Shelf Res.* **23**, 113-124.

Rutgers van der Loeff, M., Sarin, M. M., Baskaran, M., Benitez-Nelson, C., Buesseler, K. O., Charette, M., Dai, M., Gustafsson, Ö., Masque, P., Morris, P. J., Orlandini, K., Baena, A. R. y., Savoye, N., Schmidt, S., Turnewitsch, R., Vöge, I., and Waples, J. T., 2006. A review of present techniques and methodological advances in analyzing ^{234}Th in aquatic systems. *Marine Chemistry* **100**, 190-212.

Rutgers van der Loeff, M. M., Key, R. M., Scholten, J. C., Bauch, D., and Michel, A., 1995. ^{228}Ra as a tracer for shelf water in the Arctic Ocean. *Deep-Sea Res. II* **42**, 1533-1553.

Rutgers van der Loeff, M. M., Meyer, R., Rudels, B., and Rachor, E., 2002. Resuspension and particle transport in the benthic nepheloid layer in and near Fram Strait in relation to faunal abundances and ^{234}Th depletion. *Deep Sea Research Part I: Oceanographic Research Papers* **49**, 1941-1958.

Schauer, U., 2008. The expedition ARKTIS-XXII/2 of the research vessel "Polarstern" in 2007 / ed. by Ursula Schauer with contributions of the participants. *Reports on polar and marine research* **579**, 271 pp.

Schlitzer, R., 2010. Ocean Data View. *http://odv.awi.de*.

Schlosser, P., Bauch, D., Fairbanks, R., and Bönisch, G., 1994. Arctic river run-off: mean residence time on the shelves and in the halocline. *Deep-Sea Res. I* **41**, 1053-1068.

Schlosser, P., Bayer, R., Bo?nisch, G., Cooper, L. W., Ekwurzel, B., Jenkins, W. J., Khatiwala, S., Pfirman, S., and Smethie, W. M., 1999. Pathways and mean residence times of dissolved pollutants in the ocean derived from transient tracers and stable isotopes. *Science of the Total Environment* **237-238**, 15-30.

Serreze, M. C., A.Barrett, A.J.Slater, Steele, M., Zhang, J., and Trenberth, K. E., 2006. The large-scale freshwater cycle in the Arctic. *Journal of Geophysical Research* **111**, doi:10.1029/2005JC003424.

Smith, J. N., Moran, S. B., and Macdonald, R. W., 2003. Shelf-basin interactions in the Arctic Ocean based on ^{210}Pb and Ra isotope tracer distributions. *Deep-Sea Research Part I: Oceanographic Research Papers* **50**, 397.

Trimble, S. M. and Baskaran, M., 2005. The role of suspended particulate matter in ^{234}Th scavenging and ^{234}Th-derived export fluxes of POC in the Canada Basin of the Arctic Ocean *Marine Chemistry* **96**, 1 –19.

Trimble, S. M., Baskaran, M., and Porcelli, D., 2004. Scavenging of thorium isotopes in the Canada Basin of the Arctic Ocean. *Earth and Planetary Science Letters* **222**, 915-932.

Walker, S. A., Amon, R. M. W., Stedmon, C., Duan, S., and Louchouarn, P., 2009. The use of PARAFAC modeling to trace terrestrial dissolved organic matter and fingerprint water masses in coastal Canadian Arctic surface waters. *Journal of Geophysical Research* **114**, G00F06, doi:10.1029/2009JG000990.

Wassmann, P., Bauerfeind, E., Fortier, M., Fuckuchi, M., Hargrave, B., Moran, B., Noji, T., Nöthig, E.-M., Olli, K., Peinert, R., Sasaki, H., and Shevchenko, V., 2004. Particulate organic carbon flux to the arctic ocean sea floor. In: Stein, R. and MacDonald, R. W. (Eds.), *The Organic Carbon Cycle in the Arctic Ocean.* Springer-Verlag, Berlin.

Wassmann, P., Ratkova, T., Andreassen, I., Vernet, M., Pedersen, G., and Rey, F., 1999. Spring bloom development in the Marginal Ice Zone and the central Barents Sea. . *Marine Ecololy* **20**, 321-346.

Yamamoto-Kawai, M., McLaughlin, F. A., Carmack, E. C., Nishino, S., and Shimada, K., 2008. Freshwater budget of the Canada Basin, Arctic Ocean, from salinity, δ^{18}O, and nutrients. *Journal of Geophysical Research* **113**.

FIGURE CAPTIONS

Fig 1. Cruise track (red lines) with sections (S1-5) and stations sampled during Polarstern ARK XXII/2 with Atlantic inflow in the Fram Strait and Barents Sea branches (black lines) and approximate pathway of the TPD (arrows).

Fig. 2. a) ^{226}Ra as function of the f_r (fraction of river water); b) ^{226}Ra and c) ^{228}Ra as a function of Ba of all samples shallower than 100m of ARK XXII/2 (2007) distinguishing samples from the Laptev shelf (red squares with sampling depth and the symbols dot, triangle and cross identifying stations 407, 409 and 411, respectively) and samples with significant Pacific influence (open circles, as also indicated in panel a by their Pacific water fraction f_P given in %).

Fig. 3. Distribution of ^{226}Ra (dpm m^{-3}) during ARKXXII/2 compared with literature data (excluding data from the productive Chukchi shelf waters) from GEOSECS Atlantic (BROECKER et al., 1976), Cesar Ice Camp (MOORE and SMITH, 1986), TTO (KEY et al., 1992) and Smith et al. (2003).

Fig. 4. Distribution of a) ^{228}Ra (dpm m^{-3}) and b) $^{228}Ra/^{226}Ra$ ratios in surface waters, summer 2007.

Fig. 5a) ^{228}Ra as a function of salinity and b) as a function of the meteoric fraction f_r and c) $^{228}Ra/^{226}Ra$ ratio as a function of the meteoric fraction f_r for all samples of the ARK XI/1 expedition (1995) including in c) samples from the Laptev Sea (<92°N) of the ARK XXII/2

912 expedition (triangles) distinguishing shelf (bottom depth < 260m: closed symbols) and
913 offshore stations (open symbols) compared in c) with the mixing line based on 1991 data
914 from the Eurasian Basin.
915
916 Fig. 6. ^{228}Th, ^{228}Ra and ^{228}Th/^{228}Ra ratios in surface water of section 3 (left, Kara Sea to
917 Alpha Ridge) and section 4+5 (right, Alpha Ridge to Lomonosov Ridge, then over Gakkel
918 Ridge towards Laptev Sea).
919
920 Fig. 7. Distribution of ^{228}Th/^{228}Ra ratio in surface waters of ARK XXII/2 (this study) along
921 with literature data (with ranges where symbols overlap) from the Alaskan shelf (AWS,
922 TRIMBLE et al., 2004), ICEX-03 (0.55-0.73, KADKO and MUENCH, 2005), Chukchi Sea (SBI
923 spring 0.33±0.27, summer 2002 0.23±0.22, summer 2004, 0.08±0.04 LEPORE and MORAN,
924 2007), Cesar station (BACON et al., 1989), Ice Island T3 (BROECKER et al., 1973) and the
925 Nansen Basin (stations 287, 358, COCHRAN et al., 1995).
926
927 Fig. 8. a) ^{228}Ra and b) ^{228}Ra/^{226}Ra* AR as a function of f_r for surface water samples from the
928 ARK XXII/2 expedition (2007) distinguishing samples from the Laptev shelf (red squares,
929 symbols identifying stations 407-411 as in Fig. 2), samples with significant Pacific
930 component (open circles) from samples from the Nansen and Amundsen Basin (open
931 triangles), close to the Lomonosov Ridge (closed squares: Stas 312, 358, 363) and other
932 surface samples (diamonds). The mixing line drawn by eye (straight solid line) is thought to
933 represent mixing of Atlantic inflow with a hypothetical freshwater endmember excluding the
934 samples influenced by biological cycling on the Laptev shelf and is compared here with the

935 ^{228}Ra line (broken line) obtained from the Laptev Sea - Atlantic mixing line of ^{228}Ra/^{226}Ra
936 given in Rutgers van der Loeff et al. (1995) multiplied for panel a) by ^{226}Ra from eq. 1 (Fig.
937 2a).
938
939 Fig. 9. ^{228}Th vs ^{228}Ra in surface waters of ARK XXII/2 (filled symbols distinguishing TPD,
940 black diamonds; Lomonosov Ridge, black squares; Kara and Laptev shelf, blue triangles;
941 Nansen basin, red circles; north Gakkel Ridge, red squares; southern Gakkel Ridge, red
942 triangles) along with literature data (open symbols) from the Alaskan shelf (AWS, squares,
943 TRIMBLE et al., 2004), ICEX-03 (large circles, KADKO and MUENCH, 2005), Chukchi Sea
944 (SBI, small circles, KADKO and MUENCH, 2005; triangles, LEPORE and MORAN, 2007), Cesar
945 station (C, BACON et al., 1989), Ice Island T3 (T3, BROECKER et al., 1973) and the Nansen
946 Basin station studied by Cochran (N, COCHRAN et al., 1995).
947
948 Fig. 10. Observed range of ^{234}Th/^{238}U vs. ^{228}Th/^{228}Ra compared with the theoretical steady
949 state "concordia" line (KAUFMAN et al., 1981; LEPORE and MORAN, 2007) in a) shelf stations
950 of Laptev Sea (boxes, this study and CAI et al., 2010) and Chukchi Sea (distinguishing
951 summer (open symbols) and spring (closed symbols), LEPORE and MORAN, 2007) and b)
952 central Arctic for this study (Lomonosov Ridge, ^{228}Th/^{228}Ra AR 0.4-0.6; Beaufort Gyre and
953 Gakkel Ridge AR 0.8-1.0) compared with literature AR values of Cochran et al. (COCHRAN
954 et al., 1995), Trimble et al.(2004)(AWS 3: 0.30 ± 0.03 AWS 4: 0.37 ± 0.06), Bacon et al.,
955 (1989) and Kaufmann et al. (1981).
956

957 Fig. 11. $^{234}Th/^{238}U$ ratio in surface waters as a function of a) geographical location and b)
958 bottom depth, distinguishing stations over Lomonosov Ridge (open triangles) and Barents
959 shelf (x) from other stations (dots). Data of Cai et al. (2010).
960
961 Fig. 12. a) ^{228}Th vs ^{228}Ra (dpm m^{-3}) in surface waters of this study (TPD, filled symbols)
962 compared with horizontal mixing model for $\lambda_s=0$ (including results for $F_0 = 0.1$ and 0.2, thin
963 lines), 0.21 and 0.46 y^{-1}. In the case without scavenging ($\lambda_s=0$), the results approach at high
964 distance offshore the limiting AR of $\lambda_T /(\lambda_T - \lambda_R) = 1.49$ (straight broken line).
965
966 Fig. 13. Evolution of a) ^{228}Ra (parent, with arbitrary initial activity) and ^{228}Th activity and b)
967 $^{228}Th/^{228}Ra$ ratios for several values of the scavenging constant λ_s as function of time after
968 contact with the shelf source. The range compatible with measured $^{234}Th/^{238}U$ ratios is
969 shaded. At a (^{234}Th-based) scavenging rate of 0.46 y^{-1}, an AR of 0.4 is reached after 1.6 years
970 while an AR of 0.6 is incompatible with this scavenging rate. Using $\lambda_s=0.21$ y^{-1}, the AR of
971 0.4-0.6 is reached 1-2.5 y after leaving the high-scavenging shelf regime (highlighted by
972 boxes).
973
974 Fig. 14. Age (y) of shelf waters based on equation 9 and assuming a constant Th scavenging
975 rate λ_s of 0.21 y^{-1}, omitting the stations in the Atlantic inflow identified by $^{228}Ra<20$ dpm/m^3.
976 Darkest circles have a model age > 8 year.
977
978 Fig. 15. Light transmission (%) at 10m depth during expedition ARK XXII/2.
979

Fig. 16. Particulate $^{234}Th/^{238}U$ as monitored with the automatic ^{234}Th sampler.

Fig. 17. $^{228}Th/^{228}Ra$ ratio (a) compared with b) total $^{234}Th/^{238}U$ ratio (CAI et al., 2010), c) particulate $^{234}Th/^{238}U$ ratio (automatic filtration) and d) beam transmission (CTD casts) in surface water of section 3, showing enhanced suspended load and scavenging near Lomonosov Ridge.

Fig. 18 ^{228}Th vs ^{228}Ra in surface waters over the deep basins (symbols as in Fig. 9) compared with model results for the mixing model (red lines) and the advection model (black lines) assuming a Th scavenging rate λ_s of 0 (thin lines) and 0.21 y^{-1} (heavy lines).

Fig. 19. Conceptual graph of approximate location of TPD with highest ^{228}Ra concentrations during high (AO^+, as in early 1990s) and low (AO^-, as in 2007) Arctic Oscillation, the Beaufort Gyre (BG) and the inferred recirculation in the eastern Eurasian Basin (Gakkel Gyre, GG) on a map based on Rudels (2009) with Bering Strait Inflow (BSI), Fram Strait (FB) and Barents Sea Branch (BB) of Atlantic inflow, Siberian Coastal Current (SCC) and East Greenland Current (EGC).

998 Table 1. Station date, depth and position during Polarstern expedition ARK XI/1

Station ARK-XI/1-	Date	Depth	Latitude °N	Longitude °E
2	19-07-1995	151	77.523	97.065
3	22-07-1995	1982	77.704	125.910
4	24-07-1995	54	78.010	144.889
6	25-07-1995	96	78.978	147.346
7	26-07-1995	210	79.455	148.108
9	29-07-1995	75	78.655	144.122
10	30-07-1995	50	78.002	140.003
12	31-07-1995	45	77.252	135.002
16	31-07-1995	51	76.002	130.012
18	01-08-1995	95	77.597	130.008
19	01-08-1995	264	77.622	130.047
21	02-08-1995	1180	77.857	130.030
23	03-08-1995	2354	78.158	129.973
24A	05-08-1995	3263	79.314	131.518
25	07-08-1995	2670	81.135	105.559
29	10-08-1995	2222	80.900	104.742
31	11-08-1995	1588	80.780	103.440
33	12-08-1995	253	80.427	102.017
40	15-08-1995	1780	78.531	133.979
42	16-08-1995	2176	78.698	134.608
44	17-08-1995	2679	79.137	135.007
45	18-08-1995	3424	79.999	134.961
47	20-08-1995	3909	80.915	131.155
49	22-08-1995	2650	81.053	136.565
51	23-08-1995	1742	81.071	138.928
52	24-08-1995	1215	81.160	140.155
56	26-08-1995	2428	81.177	147.399
60	28-08-1995	1778	80.341	149.975
62	29-08-1995	1063	80.081	149.842
65	30-08-1995	234	79.515	148.239
71	01-09-1995	604	78.341	135.075
73	02-09-1995	107	78.247	135.392
80	06-09-1995	1244	78.768	112.732
84	07-09-1995	95	77.895	113.718
89	09-09-1995	2721	82.343	92.848
91	10-09-1995	1079	82.072	91.038
94	10-09-1995	93	81.820	90.768

999

Table 2. In-situ pump (ISP) and RaDeCC (Rosette sampling) data of ^{228}Th, ^{228}Ra and ^{224}Ra from the Laptev Shelf

station	depth	^{228}/^{226}Ra	^{226}Ra	^{228}Ra	^{228}Th			^{228}Th/^{228}Ra	depth	^{228}/^{226}Ra	^{224}Ra	^{228}Ra	^{224}Ra/^{228}Ra	^{224}Ra/^{228}Th
	m		dpm/m^3	dpm/m^3	dpm/m^3				m		dpm/m^3	dpm/m^3		
					diss	part	total							
	ISP	ISP	20-L	ISP	ISP	ISP	ISP	ISP	RADECC	RADECC	RADECC	RADECC	RADECC	
385	7	0.50 ± 0.02	81.1 ± 4.8	41 ± 3					7	0.46 ± 0.02	18.0 ± 1.8	31.1 ± 1.4	0.58 ± 0.06	
407	7	1.27 ± 0.05	71.8 ± 4.1	91 ± 6	7	1.4[b]	8	0.09	7	1.16 ± 0.03	16.7 ± 1.7	56.2 ± 1.5	0.30 ± 0.03	2.0
407	15	3.91 ± 0.18	75[a] ± 5	293 ± 24	5	0.75	6	0.02						
407	30	1.29 ± 0.05	75[a] ± 5	97 ± 8	29	1.75	31	0.32	30	0.85 ± 0.02	10.9 ± 1.1	75.7 ± 2.3	0.14 ± 0.02	0.4
407	50	0.44 ± 0.02	75[a] ± 5	33 ± 3	7	2.38	9	0.29	65	0.85 ± 0.02	21.7 ± 2.2	81.5 ± 2.3	0.27 ± 0.03	2.3
411	7	1.35 ± 0.13	79.6 ± 4.2	107 ± 12	10	1.4[b]	11	0.11	7	1.02 ± 0.04	9.7 ± 1.0	34.1 ± 1.5	0.28 ± 0.03	0.9
411	15	1.51 ± 0.15	75[a] ± 5	113 ± 14	9	0.33	9	0.08						
411	25	1.86 ± 0.19	75[a] ± 5	140 ± 17	20	1.65	22	0.15	25	1.91 ± 0.03	47.0 ± 4.7	247.1 ± 3.2	0.19 ± 0.02	2.2
411	35	1.83 ± 0.19	75[a] ± 5	137 ± 17	19	1.4[b]	20	0.15						
shelf average (Sta 407-411)					13.3		14.6	0.15			21.2		0.24	1.5
SD					8.5		8.7	0.10			15.2		0.07	0.9

a) not measured, average of shelf samples in Fig. 2a

b) not measured, average of other particulate samples

1009 Table 3. sampling depth, potential temperature, salinity, fraction of river water, and ^{226}Ra and

1010 ^{228}Ra activity with propagated 1- σ counting errors during ARK XI/1 (data available

1011 on www.pangaea.de)

Station	depth	Pot Temp	Salinity	f_r	^{226}Ra			^{228}Ra		
ARK-XI/1-	m	°C		%	dpm/m^3			dpm/m^3		
2	5	-1.19	31.38	11.24	80.0	±	6.2	-7.9	±	11.5
2	51	-1.64	33.88	4.74	91.8	±	3.0	58.2	±	5.4
2	126	-1.29	34.26	2.72	105.2	±	2.9	45.7	±	4.9
3	5				88.7	±	2.3	58.8	±	4.1
3	30				93.9	±	2.5	53.8	±	4.4
3	50				93.2	±	2.8	44.5	±	4.7
3	251				100.2	±	2.4	8.9	±	3.5
3	1500				113.6	±	1.6	8.6	±	2.2
4	5	0.13	30.88	15.53	105.3	±	6.0	180.0	±	13.3
4	30	-1.75	33.07	13.29	111.0	±	4.7	167.8	±	9.9
6	5	-1.77	33.39	8.44	93.3	±	6.0	84.7	±	11.5
7	17	-1.76	33.23	7.58	100.9	±	4.9	55.1	±	8.3
7	50			3.46	102.1	±	3.7	54.1	±	6.3
7	100	-0.8	34.33	2.16	100.2	±	5.1	44.7	±	8.5
7	150	-0.8	34.33	2.16	109.5	±	3.9	31.8	±	5.9
7	205	0.83	34.75	0.59	107.7	±	3.8	22.3	±	5.9
9	5	-1.71	32.87	12.13	96.5	±	5.1	151.5	±	10.7
9	50	-1.8	33.44	9.30	101.2	±	6.1	102.3	±	11.7
10	5	0.59	32.39	11.27	92.6	±	5.6	89.4	±	10.3
10	40	-1.67	33.08	11.09	98.0	±	5.1	110.8	±	9.8
12	5	4.12	29.91	13.92	66.6	±	5.9	87.7	±	12.0
12	31	-1.69	32.75	10.66	83.8	±	6.3	78.5	±	12.0
16	5	2.36	28.78	18.11	77.0	±	3.9	72.8	±	7.4
16	40	-1.37	33.66	4.92	103.3	±	5.6	88.0	±	10.5
18	5	2.46	28.67	16.38	75.4	±	7.4	112.0	±	15.2
19	4	-1.42	30.95	12.42	84.7	±	4.4	58.1	±	7.4
19	39	-0.98	34.21	2.80	95.1	±	4.8	52.6	±	8.3
19	99	-0.97	34.31	2.29	108.3	±	5.3	51.1	±	8.7
19	200	-0.83	34.35	2.24	99.9	±	5.7	37.7	±	9.4
19	250	-0.82	34.35	2.14	95.9	±	4.8	44.7	±	8.1
21	5	-0.98	29.81	14.31	70.4	±	4.7	56.9	±	8.7
21	51	-1.68	33.6	4.66	73.1	±	4.4	43.0	±	8.1
21	250	1.55	34.83	0.29	83.7	±	3.4	14.3	±	5.2
21	1048	-0.01	34.88	0.29	94.5	±	3.5	25.0	±	5.5
23	5	-1.14	30.31	14.12	67.6	±	3.7	52.4	±	6.7
23	51	-1.84	33.73	4.67	76.7	±	4.2	43.8	±	7.1
23	250	1.97	34.89	0.19	75.5	±	1.7	8.6	±	2.6
23	1198	-0.31	34.9	0.35	82.9	±	2.5	24.4	±	3.9
23	2198	-0.78	34.92	0.09	96.5	±	3.1	15.1	±	4.6
23	2329	-0.79	34.93	0.15	93.3	±	3.4	12.5	±	4.8
24A	10				72.7	±	5.7	51.7	±	11.0
24A	50	-1.8	33.24	5.95	79.9	±	3.7	30.9	±	6.3
24A	250	1.88	34.88	0.29	91.7	±	2.8	10.6	±	4.2

24A	1151				97.3	±	3.5	12.5	±	5.5
24A	3250	-0.74	34.94	-0.06	113.1	±	3.6	8.3	±	4.9
25	10				98.3	±	3.2	34.8	±	5.2
25	51				91.2	±	2.4	24.6	±	3.8
25	250				97.3	±	2.5	5.9	±	3.6
25	547	0.77	34.87	0.24	85.1	±	1.9	9.1	±	2.9
25	800	0.22	34.91	0.30	91.7	±	2.8	6.5	±	4.2
25	2650	-0.78	34.94	0.20	108.5	±	2.9	8.3	±	4.3
29	615	0.33	34.87	0.45	91.7	±	2.2	14.2	±	3.2
31	11	-1.28	32.53	3.62	84.0	±	3.7	35.7	±	6.0
31	50	-1.7	34.24	1.99	97.0	±	2.4	29.9	±	3.8
31	228	1.35	34.8	0.27	97.2	±	3.1	17.0	±	4.4
31	800	-0.6	34.75	0.55	98.4	±	2.9	30.6	±	4.6
31	1400	-0.49	34.8	0.54	98.8	±	2.2	20.0	±	3.4
31	1567	-0.53	34.81	0.45	102.0	±	2.6	21.0	±	3.9
33	11	-1.52	33.53	2.52	83.2	±	3.1	32.1	±	5.0
33	43	-1.59	34.39	1.64	100.0	±	3.9	26.8	±	6.1
33	111	0.39	34.74	0.74	97.9	±	3.4	25.0	±	5.2
33	203	-0.55	34.72	0.88	97.2	±	2.4	23.8	±	3.8
33	238	-0.33	34.75	0.96	91.5	±	2.9	20.2	±	4.3
40	5				79.0	±	3.3	52.3	±	5.5
40	50	-1.81	33.62	4.57	85.6	±	3.5	30.7	±	5.3
40	282	1.93	34.87	0.35	90.5	±	2.1	7.6	±	3.1
40	588	0.56	34.86	0.48	96.6	±	2.8	12.8	±	4.1
40	1759	-0.63	34.91	0.16	101.9	±	3.1	10.6	±	4.7
42	5				70.5	±	2.7	48.0	±	4.8
42	52				92.9	±	3.7	38.9	±	5.9
42	268				90.4	±	1.8	2.6	±	2.6
42	1529	-0.57	34.9	0.25	96.3	±	3.0	11.5	±	4.6
42	2138				94.7	±	2.5	9.6	±	3.6
44	11	-1.62	30.76	13.08	78.7	±	3.0	53.2	±	5.3
44	51	-1.71	33.28	5.94	83.6	±	3.0	34.9	±	4.9
44	256	1.85	34.87	0.34	96.4	±	2.2	7.5	±	3.0
44	569	0.75	34.87	0.24	88.8	±	2.7	9.4	±	4.2
44	2864	-0.77	34.93	0.20	108.7	±	3.2	5.1	±	4.6
45	5	-1.6	30.42	13.62	73.6	±	3.5	62.5	±	6.6
45	254	1.79	34.87	0.45	81.2	±	2.2	11.9	±	3.3
45	1100	-0.38	34.89	0.35	85.9	±	2.3	9.7	±	3.3
45	3407	-0.72	34.94	0.25	92.8	±	1.6	6.4	±	2.3
47	9	-1.61	31.2	11.44	69.6	±	4.4	34.0	±	7.9
47	700	0.07	34.88	0.39	92.6	±	2.7	18.5	±	4.1
47	1999	-0.75	34.92	0.15	104.2	±	3.0	6.5	±	4.2
47	3914	-0.69	34.94	0.05	106.1	±	1.9	10.5	±	2.6
49	9	-1.6	30.43	12.45	75.6	±	3.6	59.9	±	6.3
49	261				79.9	±	2.4	15.3	±	3.6
49	751	-0.08	34.86	0.09	81.7	±	2.6	24.9	±	4.0
49	2381				99.7	±	2.8	9.2	±	4.0
51	5	-1.66	31.12	11.23	75.1	±	4.4	48.8	±	7.5
51	249	1.43	34.86	0.49	79.0	±	1.8	12.7	±	2.8
51	745	0.11	34.85	0.34	76.1	±	2.6	21.8	±	4.1
51	1667				103.1	±	2.6	10.1	±	3.7
51	1725	-0.57	34.92	0.10	103.5	±	2.9	9.7	±	4.2

52	5	-1.66	31.21	11.64	68.2	±	3.9	39.8	±	6.9
52	502	0.6	34.86	0.44	79.5	±	2.0	17.4	±	3.0
52	1182	-0.38	34.89	0.30	89.0	±	2.2	19.8	±	3.3
56	13	-1.71	31.97	9.50	76.0	±	4.1	41.8	±	7.2
56	257	1.41	34.84	0.49	87.7	±	2.8	12.6	±	4.3
56	637	0.29	34.86	0.25	79.3	±	2.3	8.3	±	3.5
56	1500	-0.44	34.91	0.25	97.9	±	2.2	-2.2	±	3.1
56	2413	-0.38	34.95	0.10	128.1	±	2.8	3.4	±	3.6
60	5	-1.76	33.01	8.46	79.4	±	3.1	25.3	±	5.0
60	50	-1.73	33.25	6.81	74.0	±	7.8	19.5	±	14.8
60	750	0.07	34.86	0.44	95.7	±	2.3	14.5	±	3.2
60	1676	-0.54	34.92	0.25	113.8	±	2.2	7.0	±	3.0
60	1745	-0.43	34.94	0.24	149.2	±	2.2	9.8	±	2.8
62	10	-1.69	32.19	8.17	87.7	±	2.7	35.6	±	4.5
62	51	-1.74	33.24	5.51	90.7	±	3.3	27.0	±	5.2
62	251	1.54	34.85	0.15	94.0	±	2.7	9.6	±	3.9
62	500	0.43	34.84	0.44	84.2	±	2.4	12.0	±	3.6
62	1049	-0.18	34.88	0.15	75.1	±	1.8	16.1	±	2.8
65	9	-1.71	32.28	8.22	85.1	±	2.8	41.4	±	4.7
65	50	-1.79	33.44	7.32	97.5	±	2.8	53.5	±	4.5
65	100	-1	34.2	2.22	88.7	±	3.1	35.8	±	5.0
65	179	0.78	34.66	0.46	92.3	±	2.9	15.2	±	4.4
65	217	1.08	34.72	0.55	97.1	±	2.2	21.6	±	3.4
71	10	0.58	28.9	15.04	65.4	±	2.3	44.7	±	4.1
71	272	1.77	34.85	0.24	79.2	±	2.6	5.7	±	3.9
71	585	0.6	34.86	0.29	81.3	±	2.4	11.0	±	3.7
73	10	0.16	28.83	15.18	56.7	±	3.5	37.7	±	6.4
73	30	-1.49	33.51	5.80	74.0	±	2.8	33.9	±	4.7
73	92	-1.3	34.09	3.45	85.6	±	3.3	24.6	±	5.1
80	10	1.3	32.42	7.23	47.6	±	3.0	32.5	±	5.5
80	250	1.17	34.85	0.55	81.2	±	2.1	13.4	±	3.2
80	318	0.92	34.84	0.60	88.6	±	2.8	14.5	±	4.1
80	920	-0.52	34.84	0.44	82.1	±	2.6	20.8	±	4.0
80	1212	-0.43	34.88	0.40	88.7	±	2.8	21.9	±	4.4
84	9	-0.13	30.16	11.06	54.5	±	3.2	37.9	±	6.1
84	76	-1.38	34.02	3.70	86.4	±	3.5	43.6	±	5.8
89	5				44.9	±	3.7	10.6	±	6.4
89	230				75.0	±	2.5	7.7	±	3.8
89	902	-0.43	34.87	0.25	86.9	±	2.6	15.3	±	4.0
89	2694	-0.78	34.93	0.00	109.8	±	2.5	9.2	±	3.3
91	5				48.4	±	2.7	23.8	±	4.8
91	268	0.77	34.82	0.64	82.7	±	2.4	17.9	±	3.7
91	500	-0.33	34.85	0.64	85.3	±	2.8	22.8	±	4.6
91	1110	-0.55	34.86	0.44	91.8	±	2.9	32.0	±	4.7
94	11	-1.67	32.19	3.69	79.6	±	4.8	35.1	±	8.4
94	76	-1.36	34.52	1.24	82.1	±	1.6	36.8	±	2.7

1012

1013 Table 4. Station number, date of sampling, bottom depth, position, sampling depth, temperature, salinity, light transmission, fraction

1014 of Pacific and of river water, sample volume, ^{224}Ra (RaDeCC), ^{226}Ra and ^{228}Ra activity, ^{228}Ra/^{226}Ra ratio and ^{228}Ra/^{226}Ra* ratio

1015 (corrected for Pacific ^{226}Ra component) and the ^{228}Th/^{228}Ra ratio (from ^{224}Ra/^{228}Ra) with propagated 1-σ counting errors

1016 during ARK XXII/2 (data available on www.pangaea.de).

Station	date	Bot. Depth	Latitude	Longitude	Depth	temperature	salinity	transmission	f_P	f_r	Volume	^{224}Ra	^{226}Ra	^{228}Ra	^{228}Ra/^{226}Ra	^{228}Ra/^{226}Ra*	^{228}Th/^{228}Ra
		m	°N	°E	m	°C		%	%	%	L	dpm m^{-3}	dpm m^{-3}	dpm m^{-3}			
237	2007-07-31	276	78.997	33.995	7	-1.52	34.231		4.3	0.9	295	5.6 ± 0.6	68.9 ± 0.7	20.1 ± 1.1	0.29 ± 0.01	0.29	0.28 ± 0.03
239	2007-08-01	222	80.995	33.996	7	-0.97	32.664		0.0	1.1	295	2.7 ± 0.3	54.6 ± 0.6	19.1 ± 1.0	0.35 ± 0.01	0.35	0.14 ± 0.02
257	2007-08-05	3958	83.497	34.047	7	-1.57	33.385	91.46	0.0	0.0	292	12.8 ± 1.3	71.9 ± 0.8	16.1 ± 1.1	0.22 ± 0.01	0.22	0.79 ± 0.10
261	2007-08-11	3854	84.645	60.934	7	-1.59	33.382		0.5	2.7	293	17.2 ± 1.7	71.8 ± 1.1	17.2 ± 1.5	0.24 ± 0.02	0.24	1.00 ± 0.13
263	2007-08-11	3702	84.173	60.999	7	-1.62	33.780	91.46	2.2	1.1	295	11.0 ± 1.1	68.7 ± 0.6	13.0 ± 0.9	0.19 ± 0.01	0.19	0.85 ± 0.10
264	2007-08-12	3512	83.654	60.425	7	-1.65	33.555	91.33	4.8	0.0	292	10.2 ± 1.0	75.3 ± 0.6	15.9 ± 0.8	0.21 ± 0.01	0.21	0.64 ± 0.07
266	2007-08-13	3040	83.138	61.741	7	-1.64	33.314		0.0	1.8	295	8.1 ± 0.8	74.3 ± 0.9	19.2 ± 1.3	0.26 ± 0.01	0.26	0.42 ± 0.05
268	2007-08-14	1575	82.806	60.797	7	-1.61	32.856		0.0	2.1	295	6.6 ± 0.7	70.2 ± 0.6	16.1 ± 0.9	0.23 ± 0.01	0.23	0.41 ± 0.05
271	2007-08-15	327	82.501	60.783	7	-1.53	32.945		0.0	2.3	295	8.0 ± 0.8	70.6 ± 0.6	15.6 ± 0.9	0.22 ± 0.01	0.22	0.51 ± 0.06
272	2007-08-15	231	82.252	61.996	7	-1.53	32.945				295	8.2 ± 0.8	69.0 ± 0.6	14.7 ± 0.8	0.21 ± 0.01	0.21	0.56 ± 0.06
274	2007-08-16	1174	82.521	67.110	7	-1.37	33.745	88.37	0.3	1.1	295	8.5 ± 0.9	72.7 ± 0.7	16.2 ± 0.9	0.22 ± 0.01	0.22	0.53 ± 0.06
276	2007-08-17	680	82.083	68.960	7	-1.69	32.904		0.0	2.8	295	9.8 ± 1.0	74.9 ± 0.6	24.7 ± 0.8	0.33 ± 0.01	0.33	0.39 ± 0.04
277	2007-08-18	1526	82.392	83.832	7	-1.66	32.640	84.88	0.0	4.4	295	3.6 ± 0.4	60.4 ± 0.8	29.0 ± 1.5	0.48 ± 0.02	0.48	0.12 ± 0.01
279	2007-08-19	325	81.230	86.182	7	-1.54	31.166	88.04	0.0	6.4	295	12.4 ± 1.2	66.6 ± 1.0	46.9 ± 1.8	0.70 ± 0.02	0.70	0.26 ± 0.03
284	2007-08-20	488	82.021	86.202	7	-1.55	30.910	88.67	0.0	6.9	295	10.6 ± 1.1	65.2 ± 0.7	48.9 ± 1.3	0.75 ± 0.02	0.75	0.22 ± 0.02
285	2007-08-20	726	82.143	86.318	7	-1.62	32.517		5.7	4.8	295	6.3 ± 0.6	68.5 ± 0.8	39.8 ± 1.5	0.58 ± 0.02	0.58	0.16 ± 0.02
285[a]	2007-08-20	726	82.143	86.318	7	-1.62	32.517		5.7	4.8	590	10.5 ± 1.1	67.4 ± 0.6	41.5 ± 1.1	0.61 ± 0.01	0.61	0.25 ± 0.03
290	2007-08-21	2078	82.580	86.423	7	-1.63	33.016	88.31	2.7	0.3	590	11.2 ± 1.1	69.0 ± 0.5	15.1 ± 0.7	0.22 ± 0.01	0.22	0.75 ± 0.08
294	2007-08-22	3148	83.115	86.245	7	-1.67	33.257	83.02			590	11.7 ± 1.2	54.4 ± 0.4	12.6 ± 0.6	0.23 ± 0.01	0.23	0.93 ± 0.10
299	2007-08-23	3693	84.051	89.042	7	-1.69	32.730		5.7	4.0	590	20.9 ± 2.1	65.3 ± 0.6	20.7 ± 0.9	0.32 ± 0.01	0.32	1.01 ± 0.11
301	2007-08-24	3751	84.583	89.820	7	-1.69	32.730				590	21.9 ± 2.2	67.5 ± 0.6	25.3 ± 0.9	0.37 ± 0.01		0.87 ± 0.09
303	2007-08-25	3967	85.243	90.162	7	-1.69	33.602		0.0	10.0	590	26.3 ± 2.6	65.2 ± 0.7	27.3 ± 1.2	0.42 ± 0.01	0.42	0.96 ± 0.11
309	2007-08-27	4447	87.046	104.714	7	-1.69	31.758		6.3	11.9	590	25.6 ± 2.6	67.7 ± 0.7	36.0 ± 1.3	0.53 ± 0.02	0.54	0.71 ± 0.08
312	2007-08-29	3046	88.119	120.209	7	-1.68	31.310	89.26	8.5	11.9	590	26.8 ± 2.7	63.0 ± 0.7	39.3 ± 1.3	0.62 ± 0.02	0.64	0.68 ± 0.07

322	2007-08-31	2773	88.127	150.077	7	-1.65	30.635	88.89	20.6	14.9	590	32.9	±	3.3	87.3	±	0.9	61.5	±	1.6	0.70	±	0.02	0.75	0.53	±	0.06
326	2007-09-01	4022	88.029	170.087	7	-1.61	30.177				590	43.7	±	4.4	84.3	±	0.8	88.9	±	1.7	1.05	±	0.02		0.49	±	0.05
328	2007-09-02	3992	87.833	-170.741	7	-1.51	29.173	90.10	33.1	18.3	590	45.2	±	4.5	80.0	±	0.8	85.0	±	1.8	1.06	±	0.02		0.53	±	0.05
333	2007-09-04	3279	87.028	-146.400	7	-1.55	28.728		49.1	18.0	590	56.2	±	5.6	87.6	±	1.4	89.6	±	2.8	1.02	±	0.03	1.19	0.63	±	0.07
335	2007-09-05	2499	86.364	-139.359	7	-1.53	28.475	90.75	75.7	14.8	590	55.2	±	5.5	90.6	±	1.1	87.1	±	2.2	0.96	±	0.02	1.21	0.63	±	0.07
338	2007-09-05	1537	85.705	-135.041	7	-1.54	28.585		83.2	11.2	590	58.8	±	5.9	92.1	±	1.4	77.4	±	2.7	0.84	±	0.03	1.08	0.76	±	0.08
342	2007-09-07	2302	84.500	-138.419	7	-1.47	29.290		85.1	8.3	590	46.3	±	4.6	91.7	±	0.9	57.0	±	1.5	0.62	±	0.01	0.80	0.81	±	0.08
346	2007-09-08	2355	84.794	-149.120	7	-1.48	28.212	90.66			585	61.0	±	6.1	85.8	±	0.5	91.7	±	1.1	1.07	±	0.01		0.67	±	0.07
349	2007-09-09	2020	85.065	-164.497	7	-1.41	26.911	90.87	70.7	19.0	590	61.6	±	6.2	94.7	±	1.5	123.0	±	3.5	1.30	±	0.03	1.63	0.50	±	0.05
352	2007-09-10	4002	86.632	177.590	7	-1.59	29.524				295	47.7	±	4.8	85.2	±	1.5	83.7	±	3.2	0.98	±	0.03		0.57	±	0.06
358	2007-09-11	1459	86.506	151.963	7	-1.66	30.892	90.55	9.8	11.9	295	31.8	±	3.2	70.7	±	1.1	53.3	±	2.2	0.75	±	0.03	0.78	0.60	±	0.06
363	2007-09-12	3800	86.392	135.847	7	-1.68	31.302		10.7	11.5	295	32.1	±	3.2	67.7	±	1.1	51.5	±	2.1	0.76	±	0.02	0.79	0.62	±	0.07
371	2007-09-16	4266	84.661	102.737	7	-1.69	33.157		8.9	9.4	295	38.0	±	3.8	64.6	±	0.9	30.5	±	1.6	0.47	±	0.02	0.47	1.24	±	0.14
377	2007-09-18	4347	83.410	115.600	7	-1.57	31.193	89.62			295	35.3	±	3.5	63.7	±	0.6	37.4	±	1.2	0.59	±	0.01	0.59	0.94	±	0.10
382	2007-09-19	5345	81.358	120.719	7	-1.65	31.271		0.1	10.6	295	28.6	±	2.9	62.8	±	0.9	31.9	±	1.6	0.51	±	0.02	0.51	0.90	±	0.10
385	2007-09-20	3525	79.346	124.347	7	-0.97	31.206		0.0	7.4	285	18.0	±	1.8	67.6	±	0.8	31.1	±	1.4	0.46	±	0.02	0.46	0.58	±	0.06
389	2007-09-21	2600	78.355	124.522	7	-0.09	31.466		0.0	7.7	290	19.0	±	1.9	64.8	±	0.9	43.8	±	1.6	0.68	±	0.02	0.68	0.43	±	0.05
400	2007-09-22	1041	77.366	123.428	7	-1.60	30.723	89.47	0.0	9.5	295	19.6	±	2.0	64.8	±	0.9	49.8	±	1.7	0.77	±	0.02	0.77	0.39	±	0.04
400[b]	2007-09-22	1041	77.366	123.428	7	-1.60	30.723	89.47	0.0	9.5	295	19.1	±	1.9	67.5	±	0.9	51.2	±	1.8	0.76	±	0.02	0.76	0.37	±	0.04
400	2007-09-22	1041	77.366	123.428	20	-1.46	33.057	90.59	0.0	5.3	157	14.6	±	1.5	76.6	±	1.1	50.9	±	2.1	0.66	±	0.02	0.66	0.29	±	0.03
407	2007-09-23	75	76.181	122.139	7	-0.44	29.531	89.02	0.0	12.7	295	16.7	±	1.7	48.4	±	0.7	56.2	±	1.5	1.16	±	0.03	1.16	0.30	±	0.03
407	2007-09-23	75	76.181	122.139	65	-1.63	33.812	64.77			132	21.7	±	2.2	95.5	±	1.2	81.5	±	2.3	0.85	±	0.02	0.85	0.27	±	0.03
407	2007-09-23	75	76.181	122.139	30	-1.58	33.433	86.73	0.0	6.3	129	10.9	±	1.1	88.6	±	1.1	75.7	±	2.3	0.85	±	0.02	0.85	0.14	±	0.02
409	2007-09-23	65	75.706	121.770	7	0.78	30.073	89.07	0.0	12.8	295	10.0	±	1.0	35.4	±	0.7	41.2	±	1.4	1.16	±	0.04	1.16	0.24	±	0.03
409	2007-09-23	65	75.706	121.770	55	-1.65	33.403	77.36	0.0	9.4	146	6.8	±	0.7	108.5	±	2.0	117.1	±	4.5	1.08	±	0.04	1.08	0.06	±	0.01
411	2007-09-24	49	75.201	121.365	7	0.43	29.089	89.32	0.0	13.1	295	9.7	±	1.0	33.3	±	0.7	34.1	±	1.5	1.02	±	0.04	1.02	0.28	±	0.03
411	2007-09-24	49	75.201	121.365	40	0.01	32.655	62.43	0.0	14.5	147	13.1	±	1.3	138.3	±	1.8	242.3	±	4.9	1.75	±	0.03	1.75	0.05	±	0.01
411	2007-09-24	49	75.201	121.365	25	0.46	32.499	60.90	0.0	15.4	160	47.0	±	4.7	129.2	±	1.2	247.1	±	3.2	1.91	±	0.03	1.91	0.19	±	0.02

a) duplicate sample with double sample volume

b) duplicate sample with loose uncoated acrylic fiber instead of cartridge prefilter

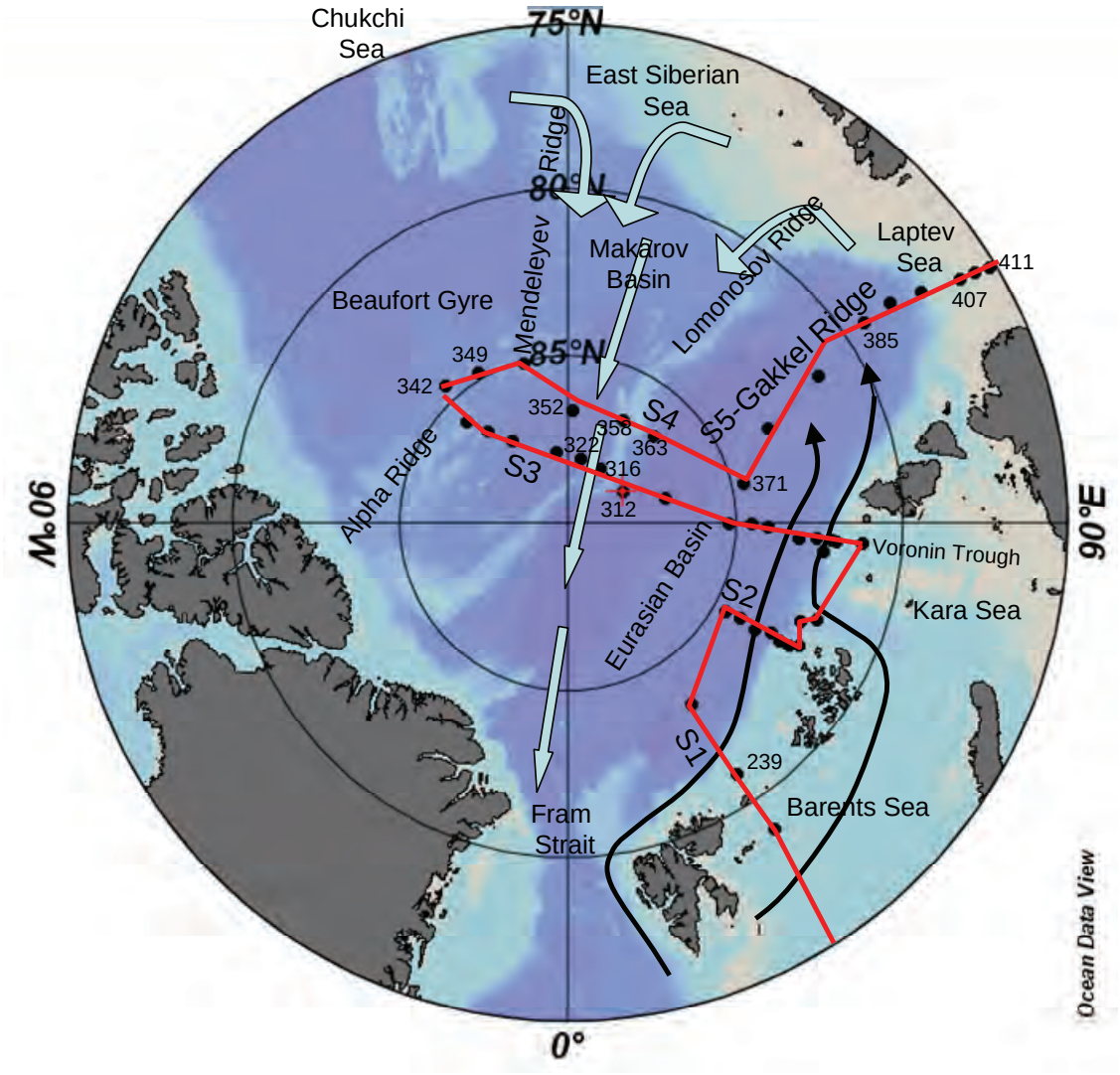
Chukchi Sea
75°N
East Siberian Sea
Ridge
80°N
Mendeleyev
Makarov Basin
Lomonosov Ridge
Laptev Sea
411
407
Beaufort Gyre
85°N
385
349
342
352
S4
S5-Gakkel Ridge
358
363
322
316
371
S3
Alpha Ridge
312
90°W
90°E
Voronin Trough
Eurasian Basin
S2
Kara Sea
S1
239
Barents Sea
Fram Strait
0°
Ocean Data View

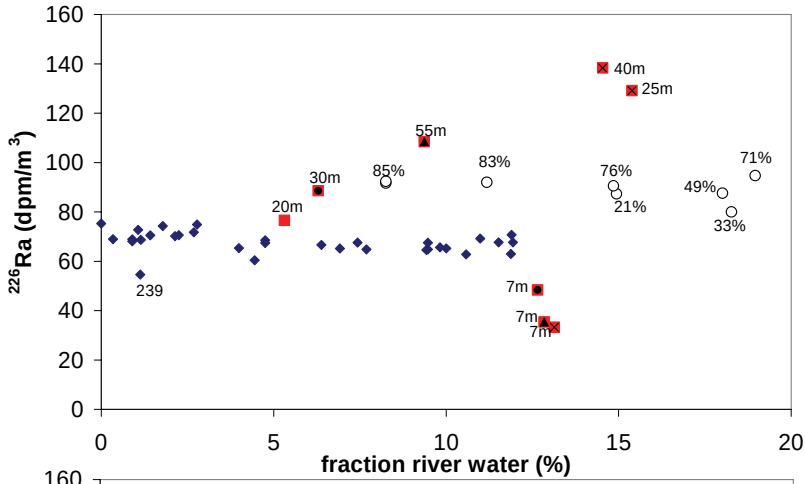
160
140
120
100
80
60
40
20
0
0
5
10
15
20
226Ra (dpm/m3)
fraction river water (%)
40m
25m
55m
30m
20m
85%
83%
76%
21%
71%
49%
33%
239
7m
7m
7m

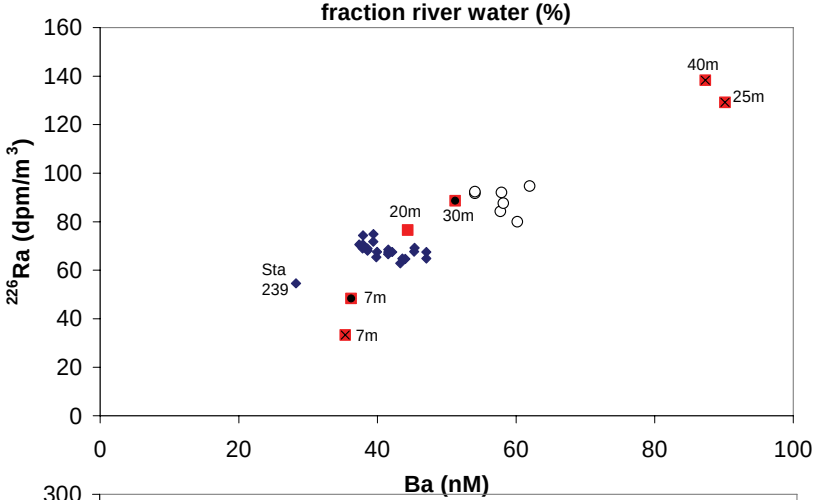
160
140
120
100
80
60
40
20
0
0
20
40
60
80
100
226Ra (dpm/m3)
Ba (nM)
40m
25m
20m
30m
Sta
239
7m
7m

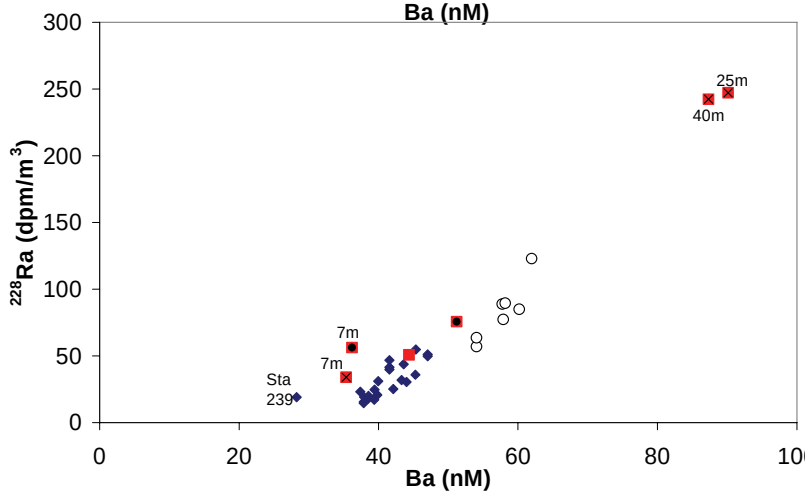
300
250
200
150
100
50
0
0
20
40
60
80
100
228Ra (dpm/m3)
Ba (nM)
25m
40m
7m
7m
Sta
239

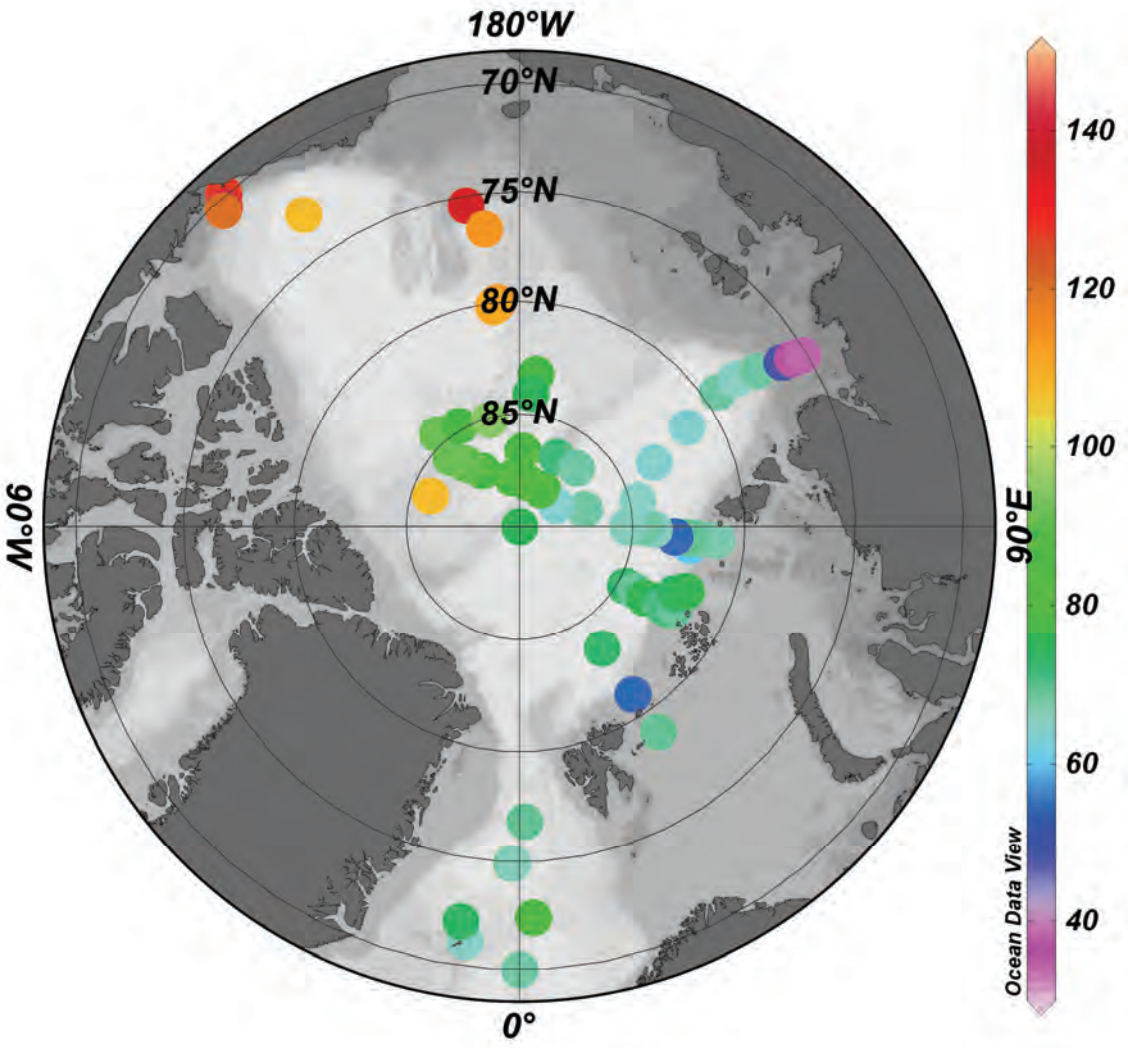
180°W
70°N
75°N
80°N
85°N
M₀06
90°E
0°
140
120
100
80
60
40
Ocean Data View

a

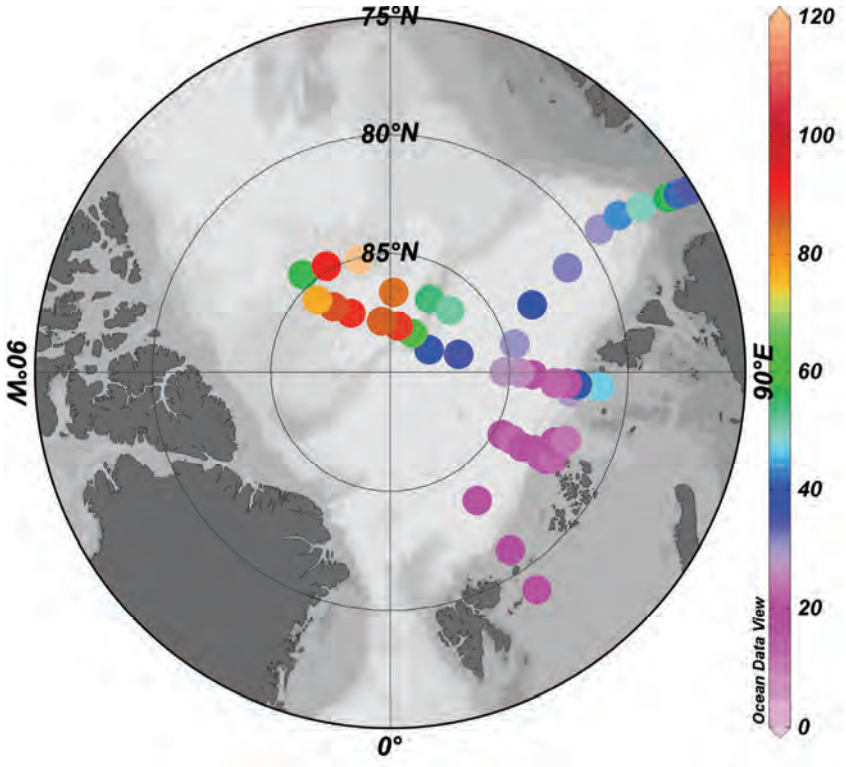
75°N
80°N
85°N
M₀06
90°E
0°
120
100
80
60
40
20
0
Ocean Data View

b

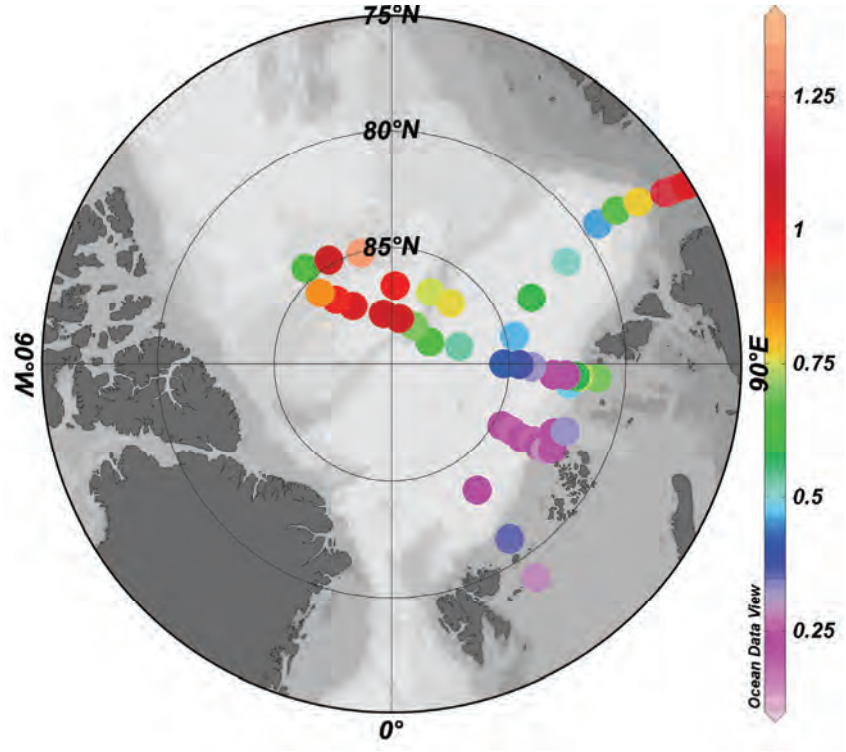
75°N
80°N
85°N
M₀06
90°E
0°
1.25
1
0.75
0.5
0.25
Ocean Data View

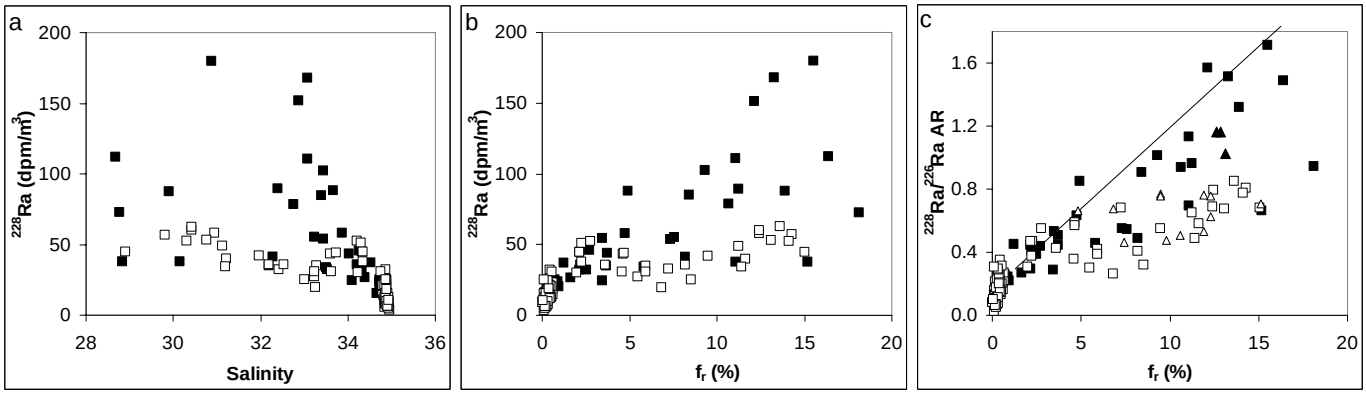
a
b
c
^{228}Ra (dpm/m^3)
Salinity
f_r (%)
^{228}Ra/^{226}Ra AR

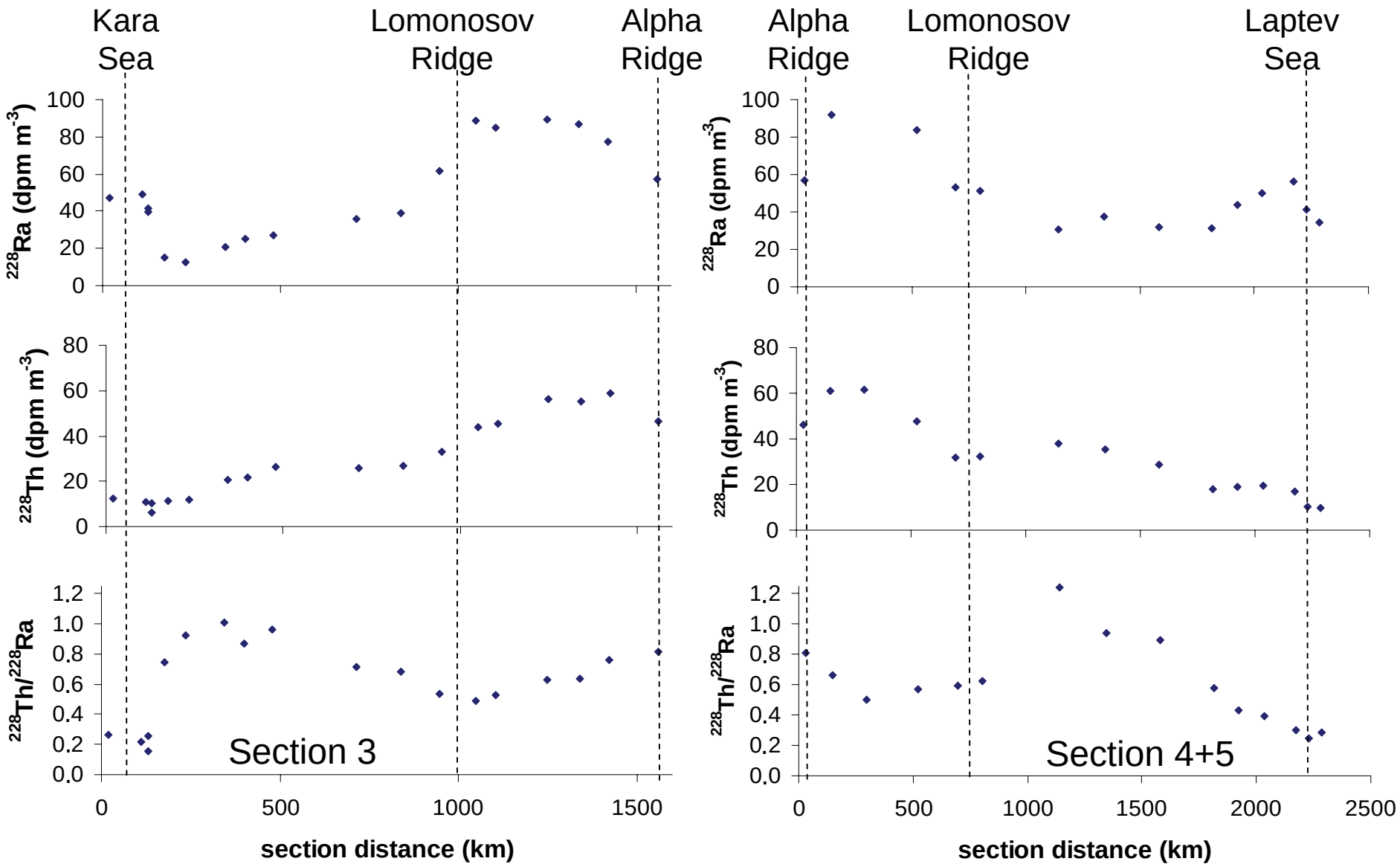
Kara Sea
Lomonosov Ridge
Alpha Ridge
Alpha Ridge
Lomonosov Ridge
Laptev Sea
228Ra (dpm m-3)
228Th (dpm m-3)
228Th/228Ra
Section 3
Section 4+5
section distance (km)
section distance (km)

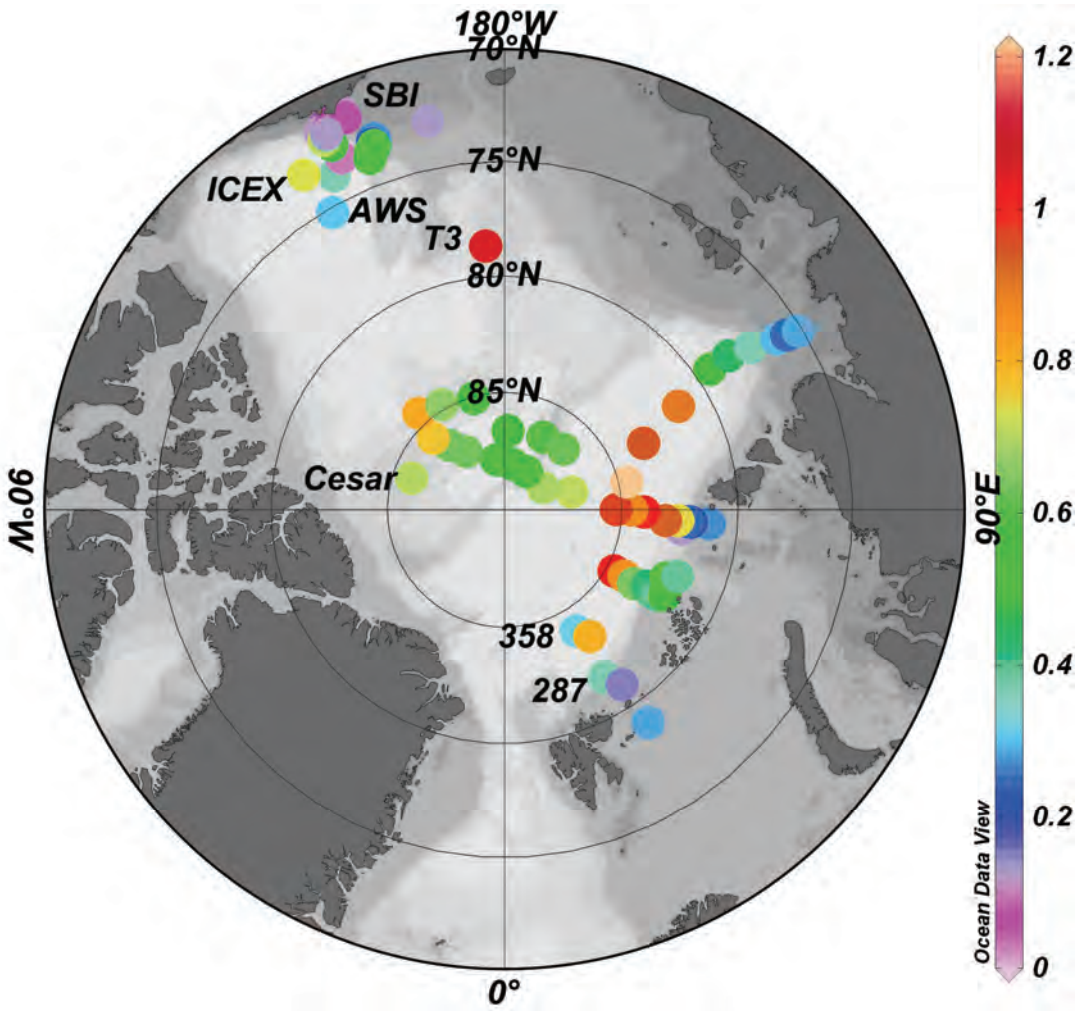
180°W
70°N
SBI
75°N
ICEX
AWS
T3
80°N
85°N
Cesar
M.06
90°E
358
287
0°
1.2
1
0.8
0.6
0.4
0.2
0
Ocean Data View

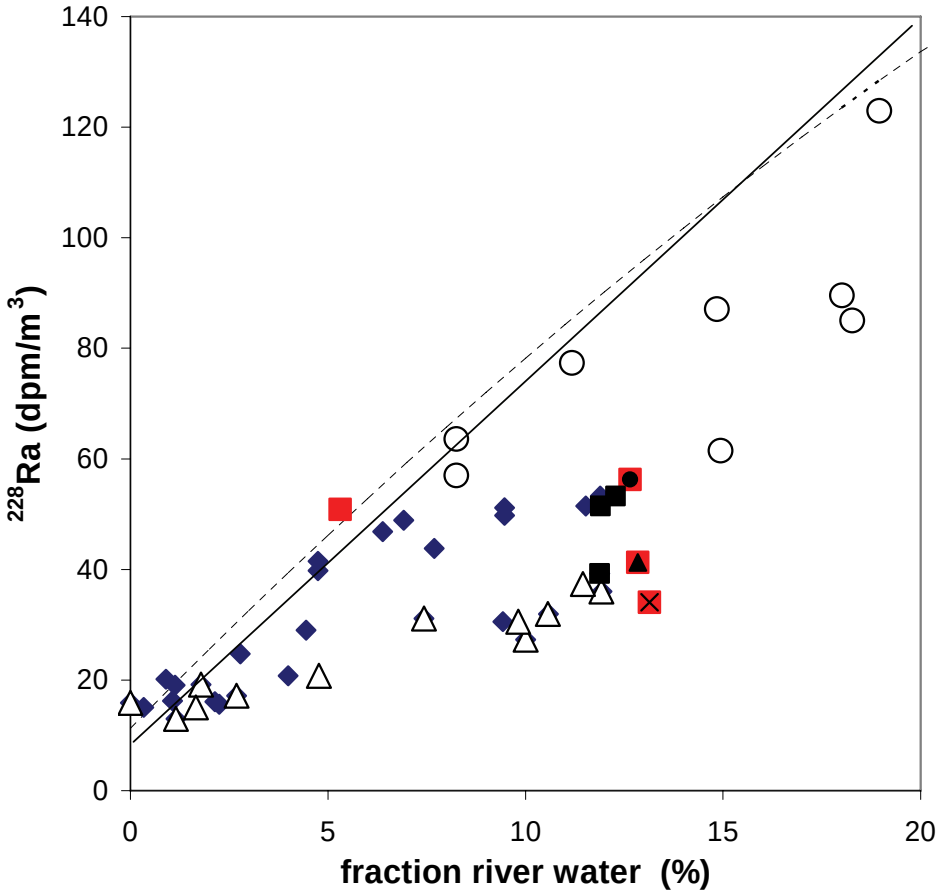
140
120
100
80
60
40
20
0
0
5
10
15
20
228Ra (dpm/m3)
fraction river water (%)

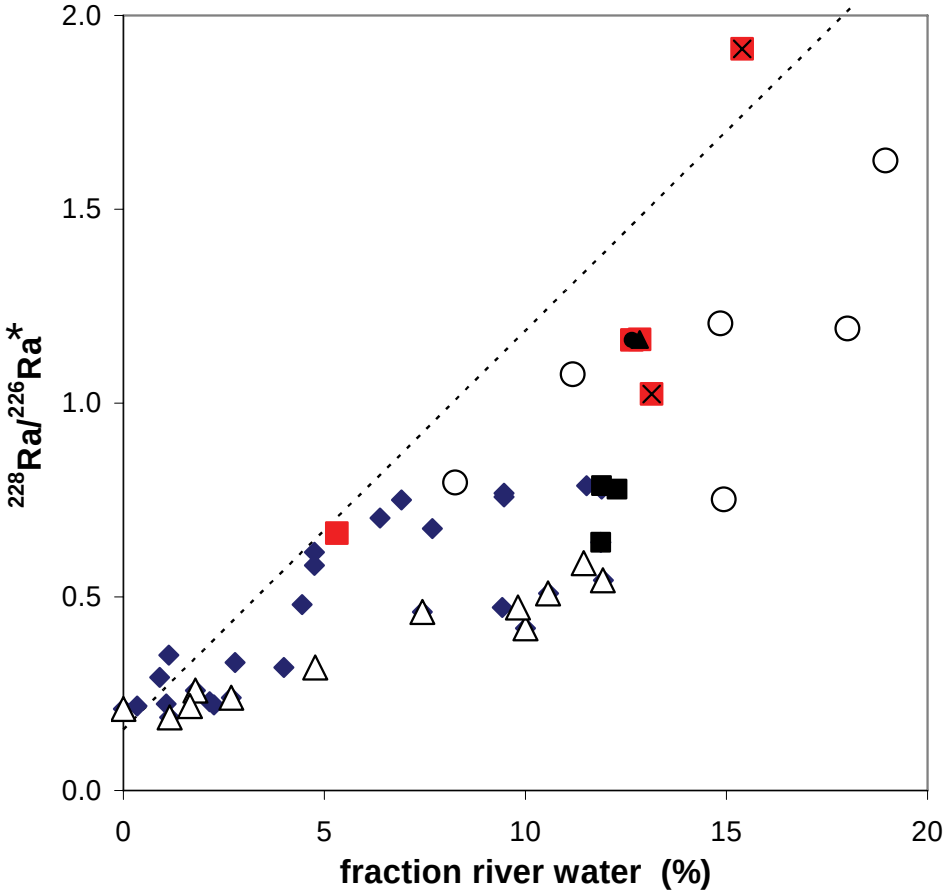
2.0
1.5
1.0
0.5
0.0
0
5
10
15
20
228Ra/226Ra*
fraction river water (%)

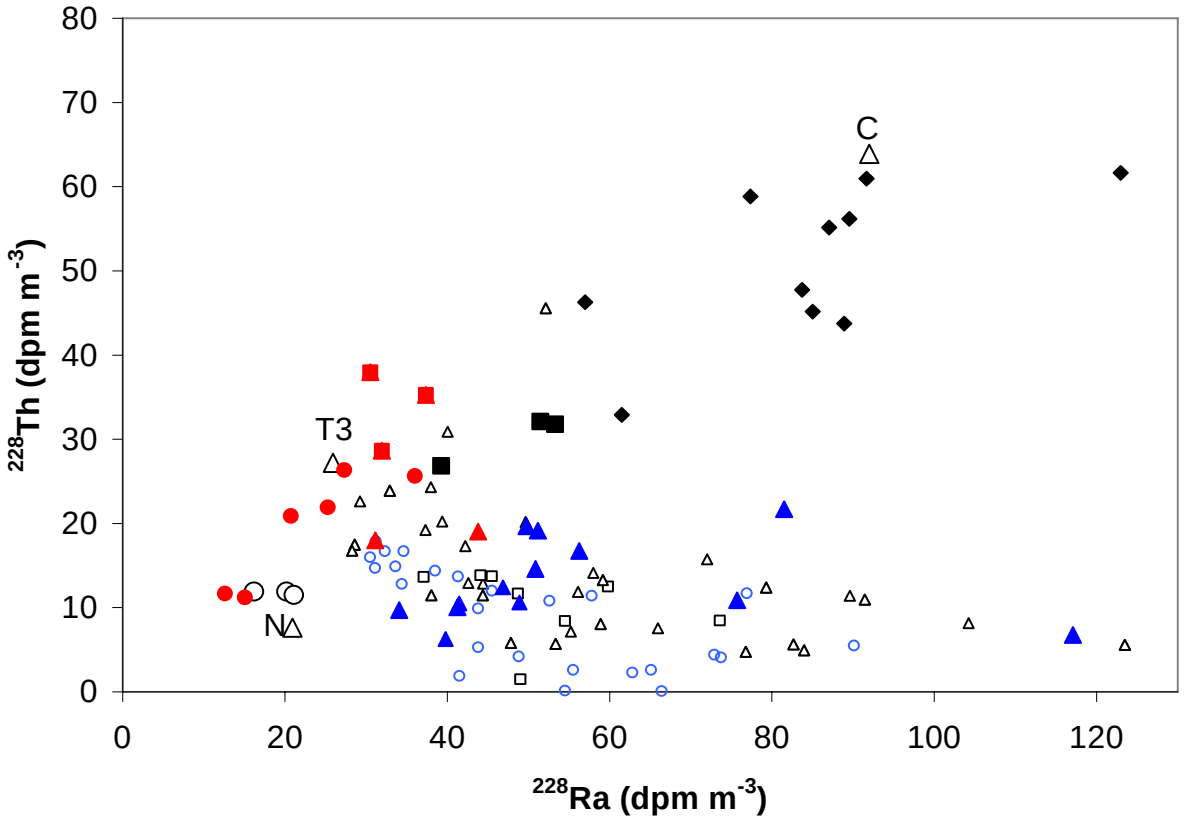
80
70
60
50
40
30
20
10
0
0
20
40
60
80
100
120
C
T3
N
228Th (dpm m-3)
228Ra (dpm m-3)

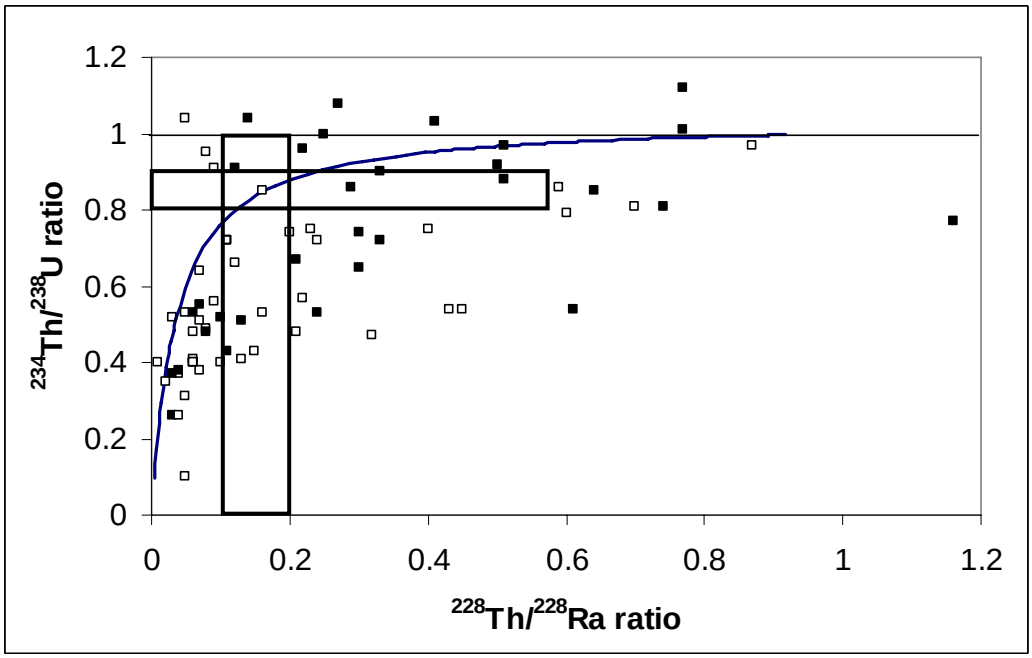
1.2
1
0.8
0.6
0.4
0.2
0
0
0.2
0.4
0.6
0.8
1
1.2
234Th/238U ratio
228Th/228Ra ratio

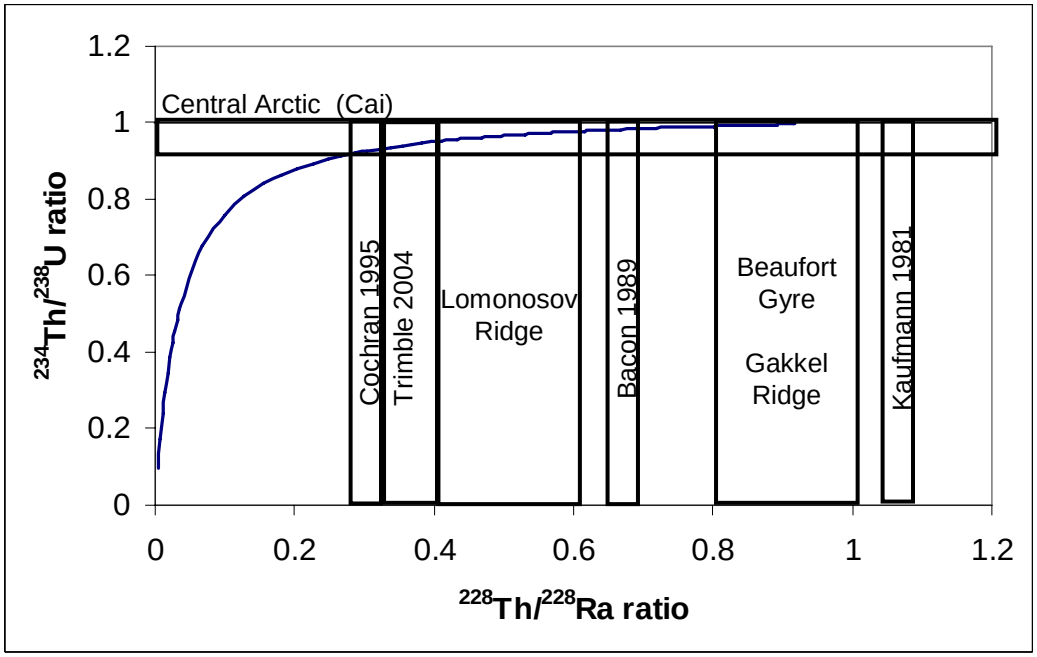
Central Arctic (Cai)
Cochran 1995
Trimble 2004
Lomonosov Ridge
Bacon 1989
Beaufort Gyre
Gakkel Ridge
Kaufmann 1981
1.2
1
0.8
0.6
0.4
0.2
0
0
0.2
0.4
0.6
0.8
1
1.2
234Th/238U ratio
228Th/228Ra ratio

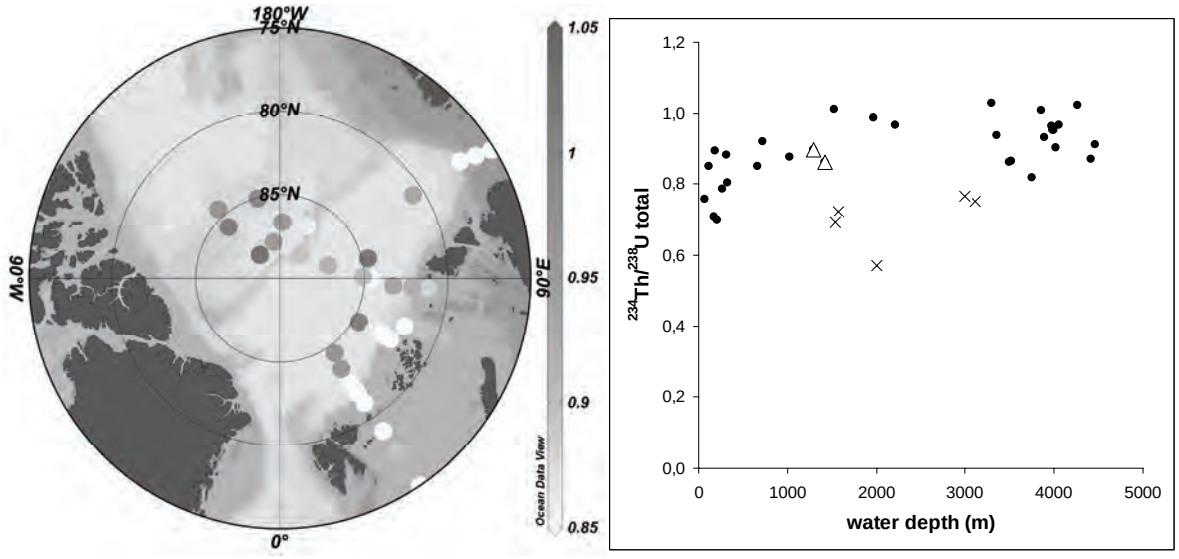
180°W
75°N
80°N
85°N
90°E
0°
M₀06
1.05
1
0.95
0.9
0.85
Ocean Data View
1,2
1,0
0,8
0,6
0,4
0,2
0,0
0
1000
2000
3000
4000
5000
water depth (m)
234Th/238U total

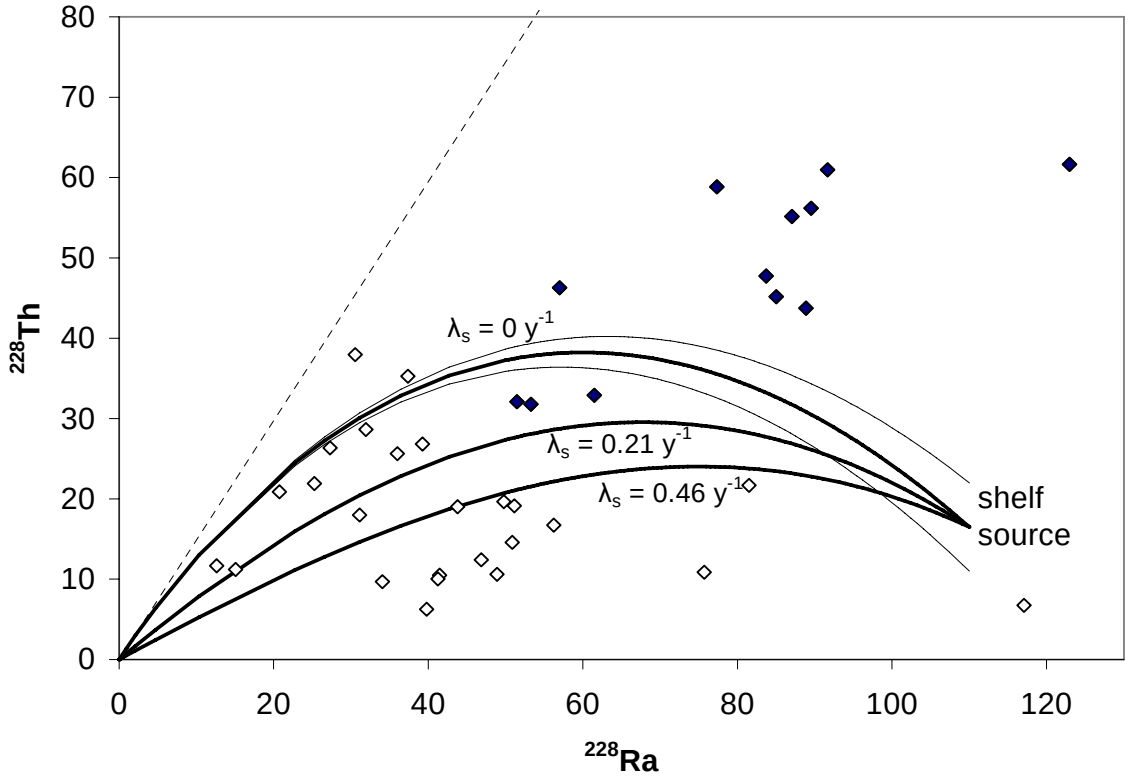
80
70
60
50
40
30
20
10
0
0
20
40
60
80
100
120
228Th
228Ra
λs = 0 y-1
λs = 0.21 y-1
λs = 0.46 y-1
shelf
source

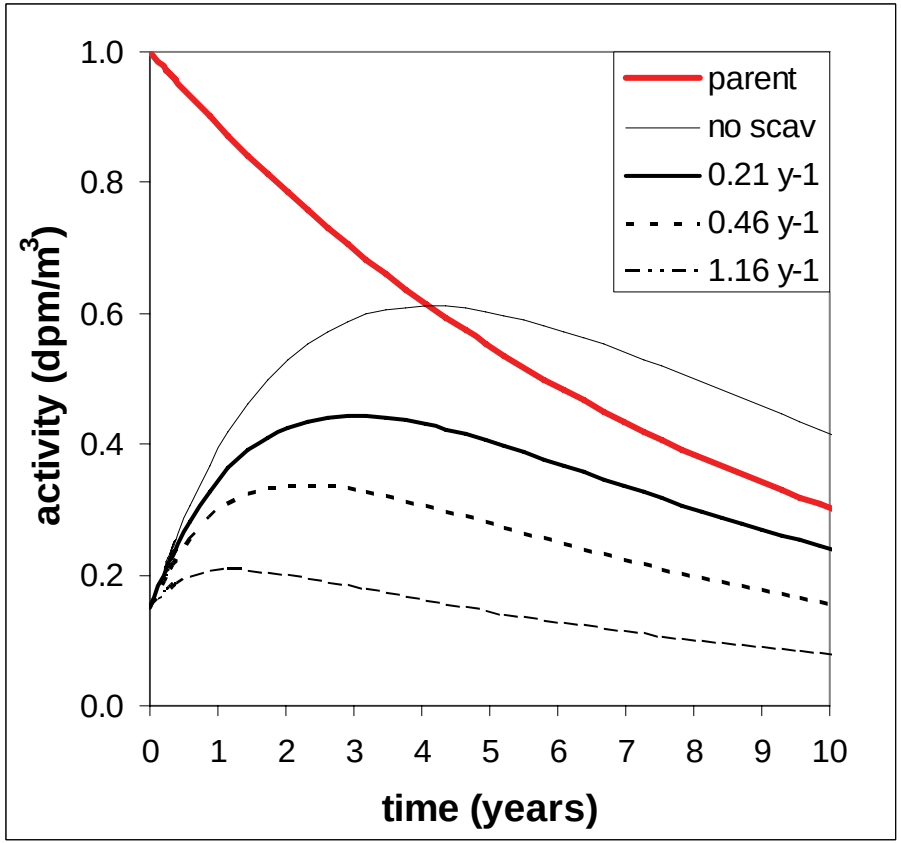
1.0
0.8
0.6
0.4
0.2
0.0
activity (dpm/m3)
0
1
2
3
4
5
6
7
8
9
10
time (years)
parent
no scav
0.21 y-1
0.46 y-1
1.16 y-1

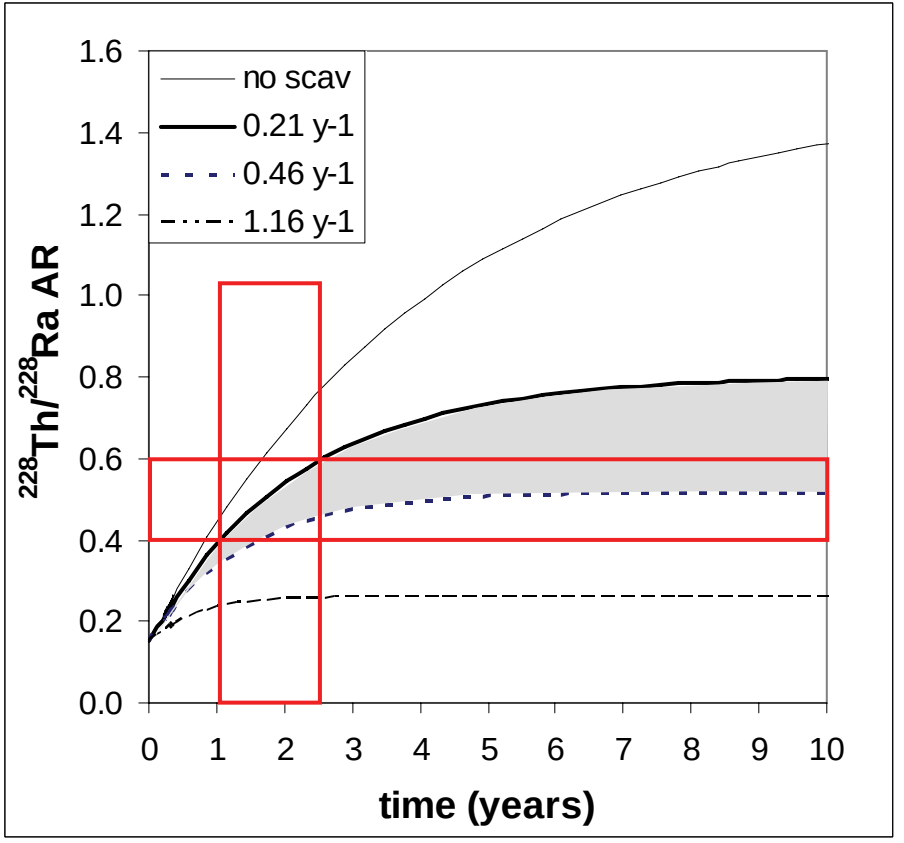
1.6
1.4
1.2
1.0
0.8
0.6
0.4
0.2
0.0
228Th/228Ra AR
0
1
2
3
4
5
6
7
8
9
10
time (years)
no scav
0.21 y-1
0.46 y-1
1.16 y-1

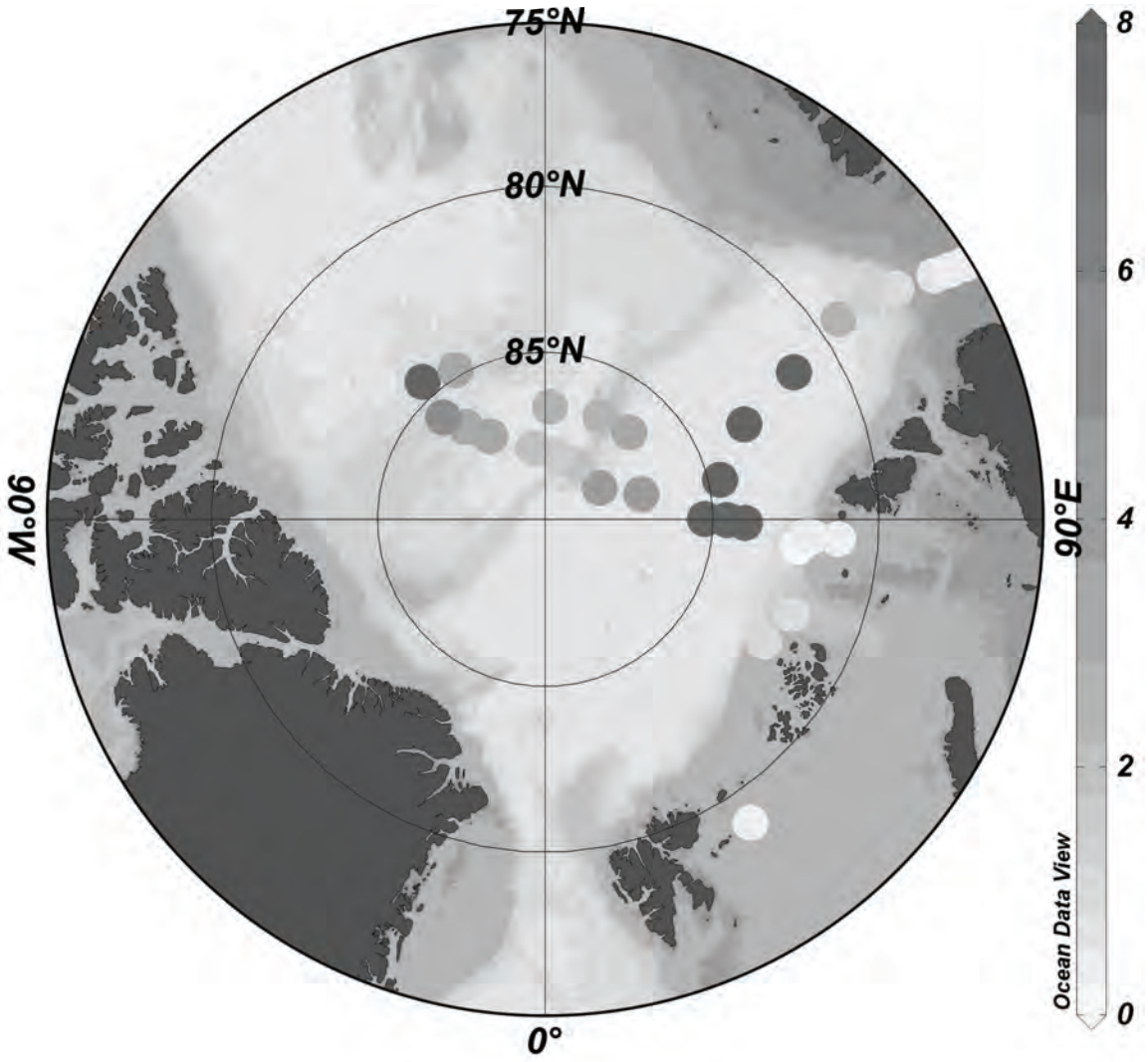
75°N
80°N
85°N
90°W
90°E
0°
8
6
4
2
0
Ocean Data View

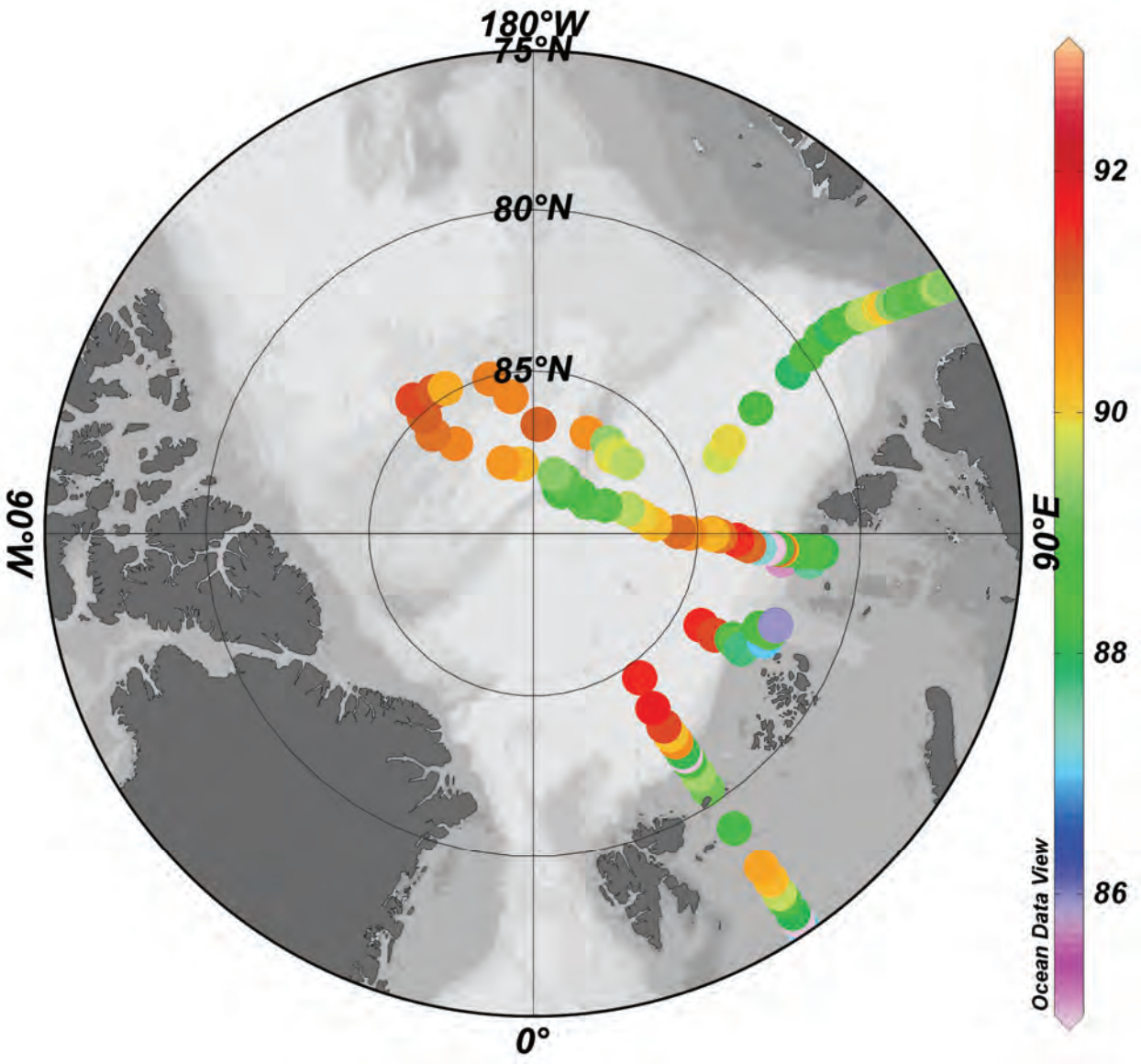
180°W
75°N
80°N
85°N
90°E
0°
M.06
92
90
88
86
Ocean Data View

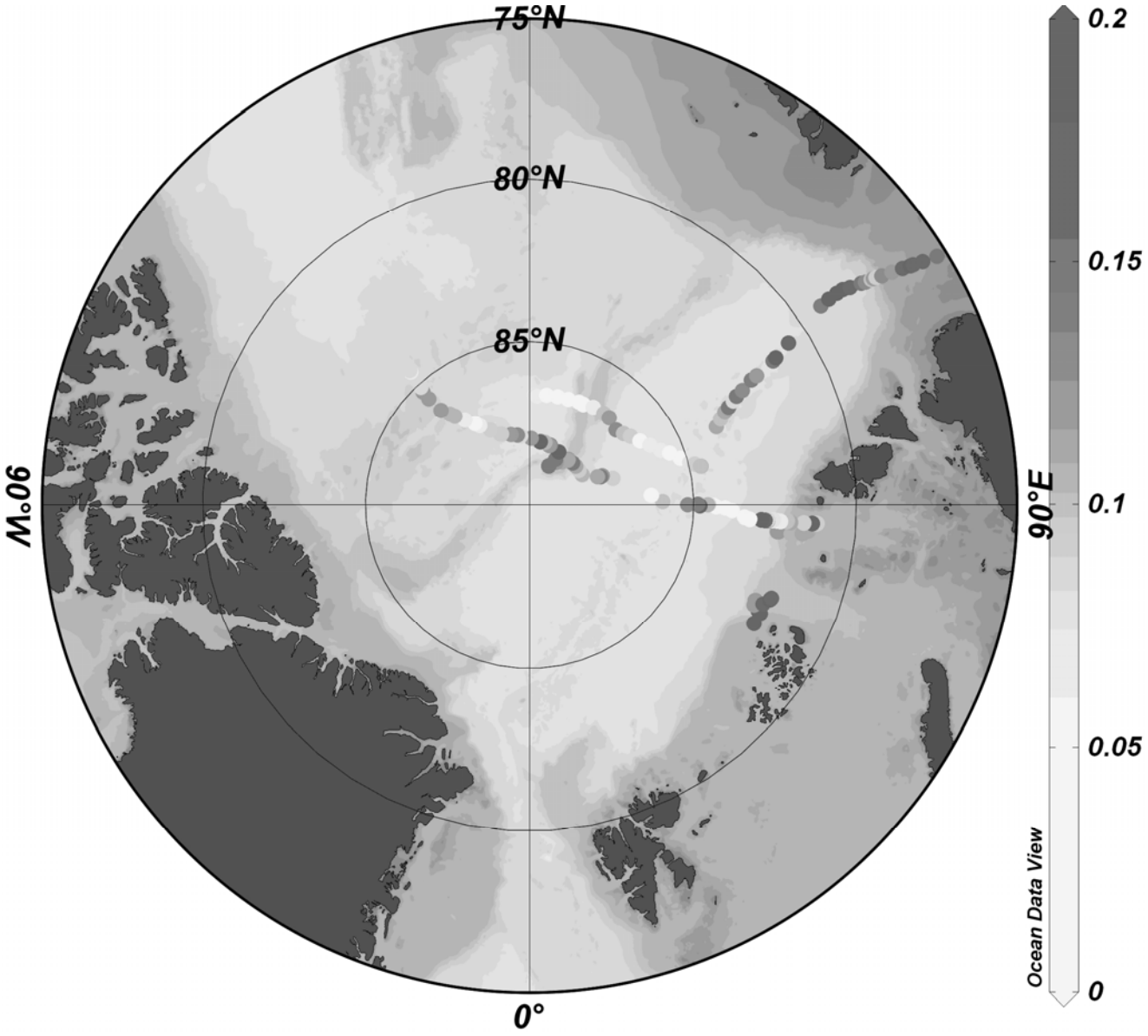
75°N
80°N
85°N
90°E
0°
M₀06
0.2
0.15
0.1
0.05
0
Ocean Data View

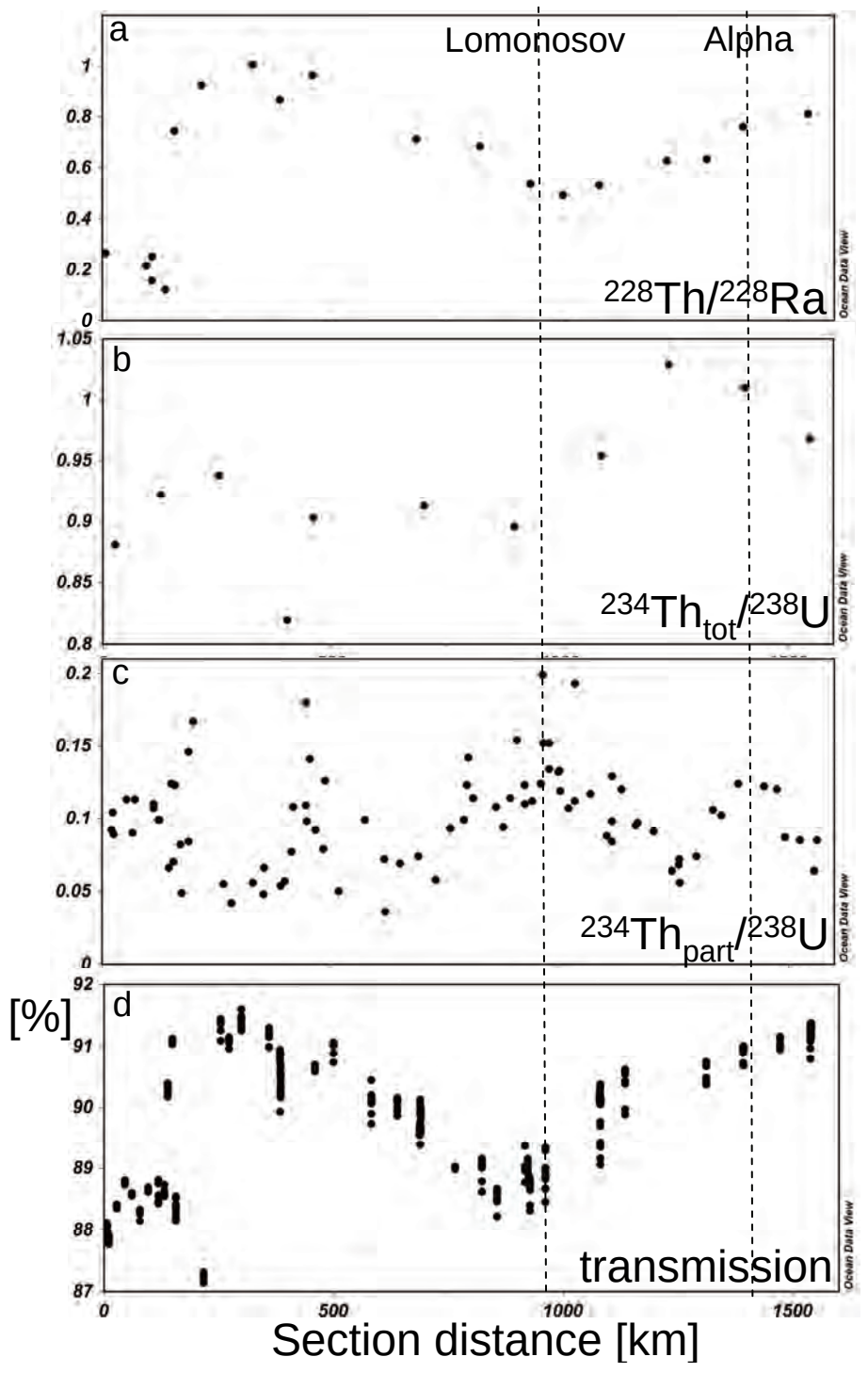
a
Lomonosov
Alpha
1
0.8
0.6
0.4
0.2
0
228Th/228Ra
Ocean Data View
b
1.05
1
0.95
0.9
0.85
0.8
234Th tot/238U
Ocean Data View
c
0.2
0.15
0.1
0.05
0
234Th part/238U
Ocean Data View
[%]
d
92
91
90
89
88
87
transmission
Ocean Data View
0
500
1000
1500
Section distance [km]

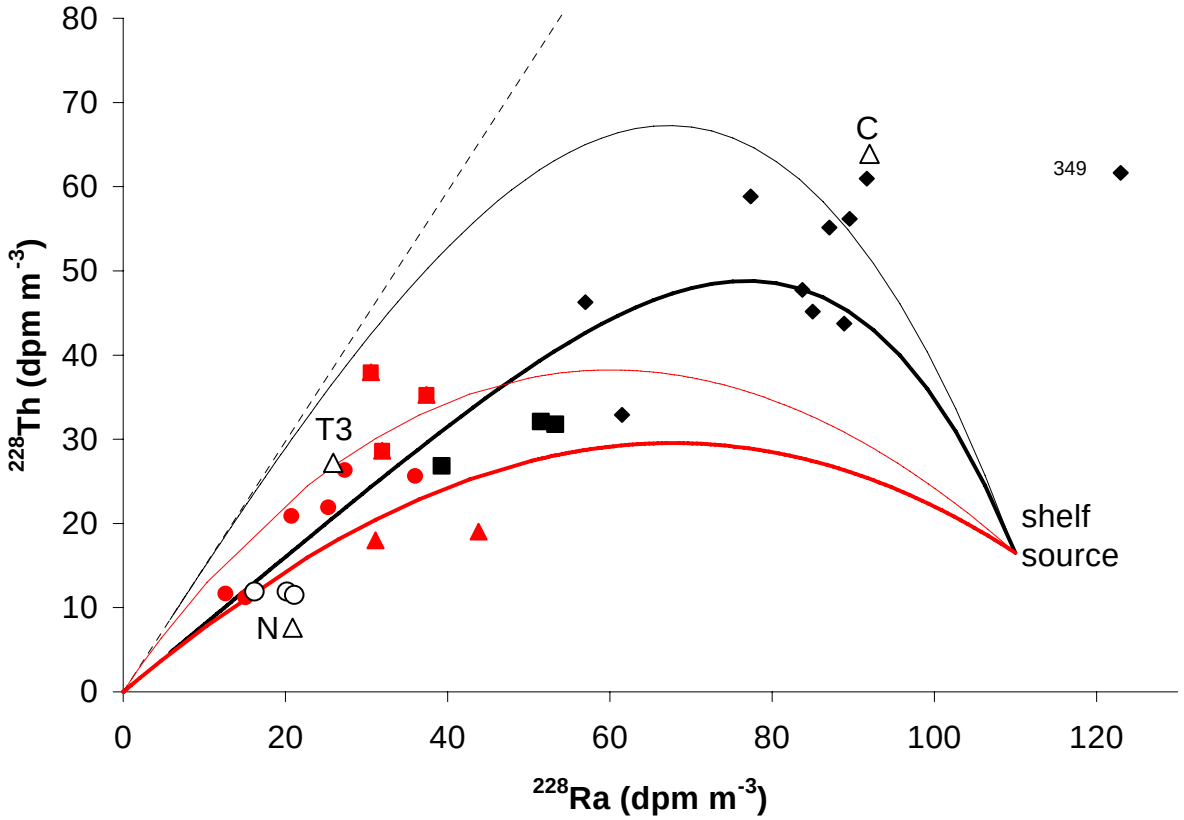
80
70
60
50
40
30
20
10
0
0
20
40
60
80
100
120
228Th (dpm m-3)
228Ra (dpm m-3)
C
T3
N
shelf
source
349

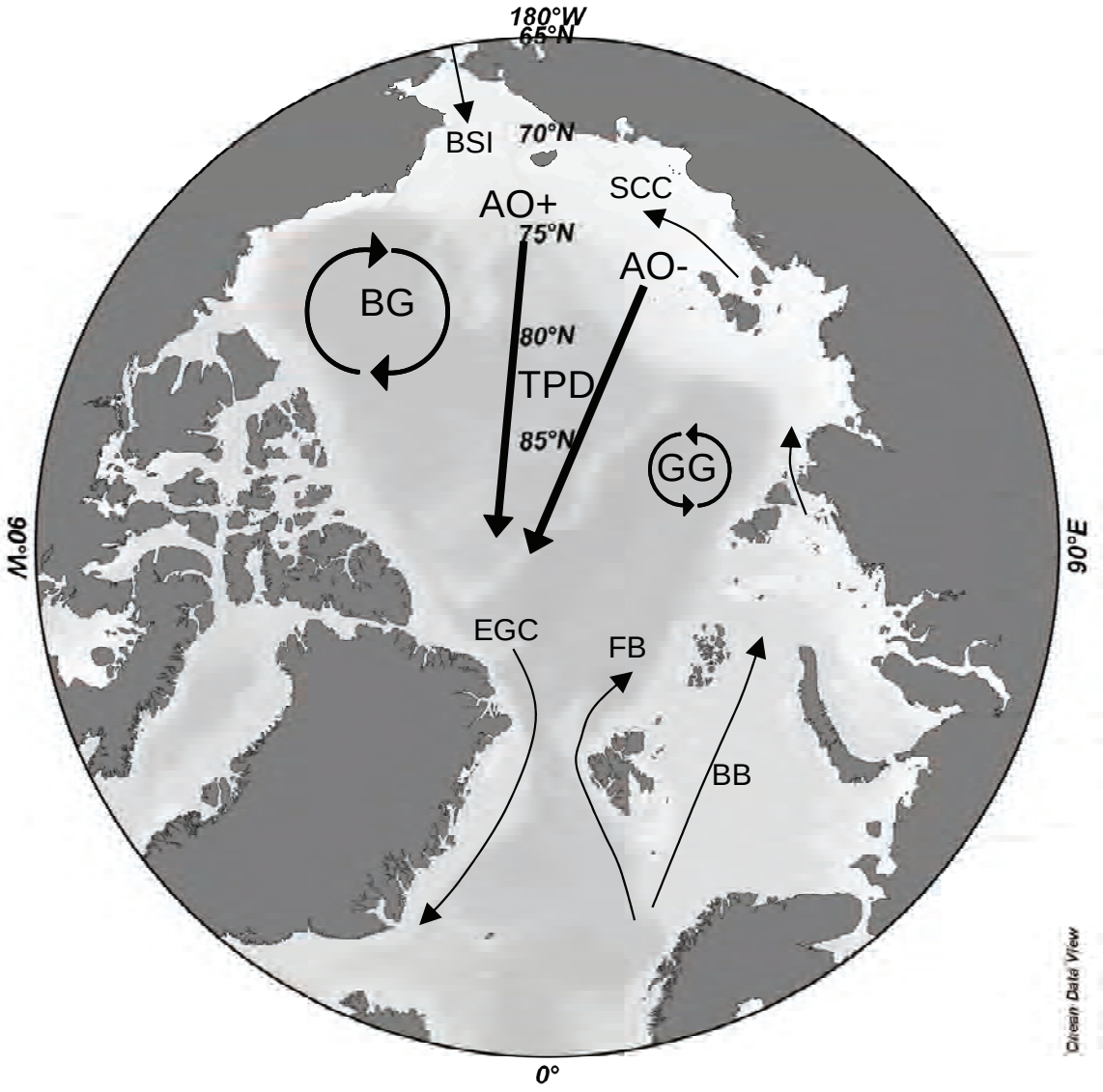
180°W
65°N
BSI
70°N
AO+
SCC
75°N
AO-
BG
80°N
TPD
85°N
GG
90°E
EGC
FB
BB
0°
Ocean Data View